

Hybrid Energy System Reference Designs for Steel, Ammonia, and Hydrogen Production

Jared J. Thomas, Kaitlin Brunik, Mariya N. Koleva, Elenya Grant, Evan P. Reznicek, Christopher Bay, and Jennifer King

National Renewable Energy Laboratory

This is a temporary cover page. A final cover page will be generated by comms with current style and formatting.

v2.0.5, March 2024

Executive Summary

This report provides details for five reference hybrid energy systems for steel, ammonia, and hydrogen production. The purpose of these reference designs is to provide a common point of comparison as well as a starting point for academia and industry in their own hybrid system development and research efforts. Individual sites were selected based on regional environmental and economic considerations. The selected reference design locations are in Minnesota, Texas, the New York Bight, and California; two sites are in Texas. Two of the reference designs are located fully onshore (Minnesota and Texas), and three of the reference designs are split, with the wind energy plant located offshore and the remainder of the system located onshore (New York Bight, California, and Texas Gulf Coast). Two of the offshore wind plants use fixed foundations, and the California plant uses floating foundations for the wind turbines.

Reference plant subsystem sizing was determined through a combination of optimization and design space exploration approaches, beginning from the plants used in Reznicek et al. (2024). From this starting point we performed a coarse full-factorial exploration of the possible subsystem rating combinations and ran an optimization for the levelized cost of the final product from the best result of the full-factorial sweep. A portion of high-level information about the final reference designs is shown in Table ES-1.

Table ES-1. Overview of Reference Hybrid Energy System Designs

ID	01	02	03	04	05
State	Minnesota	Texas	Texas	New Jersey	California
Area			Gulf Coast	New York Bight	
Product	Steel	Ammonia	Hydrogen	Hydrogen	Hydrogen
On/Offshore	Onshore	Onshore	Offshore	Offshore	Offshore
PEM electrolyzer rating (MW)	720.0	640.0	1,125.0	1,125.0	1,125.0
Wind farm rating (MW)	930.0	888.0	986.0	990.0	990.0
Solar PV rating (MW)	800.0	400.0	1,500.0	1,500.0	1,500.0
Total generation rating (MW)	1,730.0	1,288.0	2,486.0	2,490.0	2,490.0
Battery power rating (MW)	108.0	0.1	375.7	375.7	375.7
Battery energy rating (MWh)	108.0	0.1	1,500.0	1,500.0	1,500.0
Hydrogen generation rating (kt)	115.0	103.0	181.0	181.0	181.0
Hydrogen storage capacity (kt)	1.7	3.4	5.3	6.6	8.2
Steel capacity (Mt/yr)	1.0				
Ammonia capacity (kt/yr)		329.0			
LCOH (USD/kg-H ₂)	6.3	4.8	9.6	10.3	14.2
LCOS (USD/t steel)	1,191.0				
LCOA (USD/kg-NH ₃)		1.1			

While the information shown in Table ES-1 is high level, these reference designs are unique in the amount of detail included. We sought to include a high-level of detail for subsystems, including wind turbine specifications, land usage, individual feedstocks, and other information. We have also included a detailed financial model of each system for the life of the plant and a breakdown for the levelized product cost. The product costs shown are determined using a cash flow analysis over the full life of the plant, including required returns on equity.

The reference designs indicate what capacities may be necessary to achieve the desired operational scale, and they also highlight the need for continued cost reductions and technological improvements. Without tax incentives and/or technological improvements, these systems are not likely to be cost competitive. However, we hope that the reference designs will be useful for comparison and research and as a starting point for those interested in industrial energy via renewable hydrogen. We expect such efforts to lead to improved technology, better system designs, and reduced product costs.

Acknowledgments

This work was authored by the National Renewable Energy Laboratory, operated by Alliance for Sustainable Energy, LLC, for the U.S. Department of Energy (DOE) under Contract No. DE-AC36-08GO28308. Funding provided by U.S. Department of Energy Office of Energy Efficiency and Renewable Energy Hydrogen and Fuel Cell Technologies Office and Wind Energy Technologies Office. The views expressed in the article do not necessarily represent the views of the DOE or the U.S. Government. The U.S. Government retains and the publisher, by accepting the article for publication, acknowledges that the U.S. Government retains a nonexclusive, paid-up, irrevocable, worldwide license to publish or reproduce the published form of this work, or allow others to do so, for U.S. Government purposes.

The authors acknowledge their collaborators in developing the framework i.e., Lawrence Berkeley National Laboratory, Argonne National Laboratory, and Oak Ridge National Laboratory and the assistance of their colleagues from the National Energy Technology Laboratory (NETL), in particular Dr. David Morgan, who provided guidance and support in deriving the CO₂ storage costs in this work.

Acronyms

ATB	Annual Technology Baseline
BOL	beginning of life
DRI	direct reduction iron
EAF	electric arc furnace
EOL	end of life
FLORIS	FLow Redirection and Induction in Steady state
GHG	greenhouse gas
GreenHEART	Green Hydrogen Energy and Renewable Technology
HDSAM	Hydrogen Deliver Scenario Analysis Model
HOPP	Hybrid Optimization and Performance Platform
HVAC	high-voltage alternating current
HVDC	high-voltage direct current
LCOA	levelized cost of ammonia
LCOH	levelized cost of hydrogen
LCOS	levelized cost of steel
NREL	National Renewable Energy Laboratory
ORBIT	Offshore Renewables Balance-of-System and Installation Tool
PEM	proton exchange membrane
PV	photovoltaics
PySAM	Python package of the System Advisor Model
SNOPT	Sparse Nonlinear OPTimizer
XDSM	eXtended Design Structure Matrix

Table of Contents

Executive Summary	iv
Acknowledgments	v
Acronyms	vi
1 Introduction	1
1.1 Industrial Energy	1
1.2 Hybrid Systems	1
1.3 The Role of Reference Designs, Use Cases, and Examples	1
1.4 Model Availability	1
2 Reference Design Development	2
2.1 Onshore Systems	2
2.2 Offshore Systems	3
2.3 Site Selection	4
2.4 Design Tools and Methods	4
2.5 Design Space Exploration	5
3 Reference System Designs	8
3.1 Common Subsystem Assumptions and Designs	8
3.1.1 Wind	8
3.1.2 Solar PV	11
3.1.3 Battery Storage	11
3.1.4 Electrolysis PEM	14
3.1.5 Hydrogen Storage	14
3.1.6 Ammonia	15
3.1.7 Steel	15
3.1.8 Reference Design Costs	15
3.2 Reference Design Overview	17
3.3 Minnesota (Onshore/Steel)	21
3.4 Texas (Onshore/Ammonia)	28
3.5 Texas, Gulf Coast (Fixed Offshore Wind With Onshore Hydrogen)	34
3.6 New York Bight (Fixed Offshore Wind With Onshore Hydrogen)	38
3.7 California (Floating Offshore Wind With Onshore Hydrogen)	42
References	49

List of Figures

Figure 1. Onshore system XDSD diagram	2
Figure 2. Simplified flowchart of a hydrogen-based steel-making process	3
Figure 3. Simplified flowchart of the Haber-Bosch process loop	3
Figure 4. Offshore system XDSD diagram	4
Figure 5. Wind resource map	5
Figure 6. Solar resource map	6
Figure 7. Geologic storage resource map	7
Figure 8. Wind turbine performance curves	8

Figure 9.	Minnesota (onshore wind to steel) system layout	21
Figure 10.	Capital expense breakdown for the electricity and hydrogen portions of Reference Design 01 . . .	22
Figure 11.	Capital expense breakdown for the steel plant portion of Reference Design 01	22
Figure 12.	Levelized cost of hydrogen breakdown for Reference Design 01	23
Figure 13.	Levelized cost of steel breakdown for Reference Design 01	24
Figure 14.	Cash flow for electricity and hydrogen portions of Reference Design 01	24
Figure 15.	Cash flow for the steel plant portion of Reference Design 01	25
Figure 16.	Renewable electricity generation and usage for Reference Design 01	26
Figure 17.	Hydrogen flow for Reference Design 01	27
Figure 18.	Texas (onshore wind to ammonia) system layout	28
Figure 19.	Capital expense breakdown for the electricity and hydrogen portions of Reference Design 02 . . .	29
Figure 20.	Capital expense breakdown for the ammonia plant portion of Reference Design 02	29
Figure 21.	Levelized cost of hydrogen breakdown for Reference Design 02	30
Figure 22.	Levelized cost of ammonia breakdown for Reference Design 02	31
Figure 23.	Cash flow for electricity and hydrogen portions of Reference Design 02	32
Figure 24.	Cash flow for the ammonia plant portion of Reference Design 02	32
Figure 25.	Renewable electricity generation and usage for Reference Design 02	33
Figure 26.	Hydrogen flow for Reference Design 02	34
Figure 27.	Texas (offshore wind to hydrogen) system layout	35
Figure 28.	Capital expense breakdown for Reference Design 03	35
Figure 29.	Levelized cost of hydrogen breakdown for Reference Design 03	36
Figure 30.	Cash flow for Reference Design 03	36
Figure 31.	Renewable electricity generation and usage for Reference Design 03	37
Figure 32.	Hydrogen flow for Reference Design 03	38
Figure 33.	Texas (offshore wind to hydrogen) system layout	39
Figure 34.	Capital expense breakdown for Reference Design 04	39
Figure 35.	Levelized cost of hydrogen breakdown for Reference Design 04	40
Figure 36.	Cash flow for Reference Design 04	40
Figure 37.	Renewable electricity generation and usage for Reference Design 04	41
Figure 38.	Hydrogen flow for Reference Design 04	42
Figure 39.	Texas (offshore wind to hydrogen) system layout	43
Figure 40.	Capital expense breakdown for Reference Design 05	43
Figure 41.	Levelized cost of hydrogen breakdown for Reference Design 05	44
Figure 42.	Cash flow for Reference Design 05	44
Figure 43.	Renewable electricity generation and usage for Reference Design 05	45
Figure 44.	Hydrogen flow for Reference Design 05	46

List of Tables

Table 1.	High-level wind turbine design specifications	9
Table 2.	Wind balance of plant power losses	9
Table 3.	Offshore Cable Specifications	10
Table 4.	Equipment Included on Offshore Substation for HVAC and HVDC Export	10
Table 5.	Reference PV Module Design Specifications	11
Table 6.	2030 Utility-Scale PV System Costs in 2022 USD	11
Table 7.	Battery parameters	12
Table 8.	Battery capacity vs. temperature	12
Table 9.	1-MW PEM Electrolyzer Model Parameters	14
Table 10.	Hydrogen storage cost model coefficients	14
Table 11.	Ammonia Cost Coefficients	15
Table 12.	Ammonia Plant Feedstock Consumption and Cost	15
Table 13.	Steel Plant Cost Coefficients	16
Table 14.	Steel Plant Feedstock/Byproduct Consumption/Production	16
Table 15.	Estimated annual average grid retail prices	17
Table 16.	Minnesota steel plant feedstock transportation costs	17
Table 17.	Overview of Reference Designs	18
Table 18.	Financial Assumptions	19
Table 19.	Normalized costs for individual subsystems. Values marked with an asterisk (*) were determined during the simulation as functions of other inputs.	20

1 Introduction

1.1 Industrial Energy

This report details several designs for different hydrogen-based end uses. Detailed parameters and associated code have been developed to provide a detailed plant design for a specified location in the U.S.

Recent advances in electrolysis technology and renewable electricity generation have made it more feasible to develop system designs with hydrogen production for industrial products such as steel and ammonia. For example, between 2010 and 2021, the global weighted average total installed cost for utility-scale solar photovoltaic (photovoltaics (PV)) and land-based wind projects plummeted 82% and 35%, respectively. (International Renewable Energy Agency 2022). Also, the cost of water electrolyzers is expected to decrease approximately 10 times, to \$150 per kilowatt, in a decade (Satyapal 2022). Further, the Inflation Reduction Act offers significant tax credits for many technologies, including hydrogen production and carbon capture, storage and sequestration. As such, renewable electricity generation combined with hydrogen production may provide cost-effective hydrogen-based feedstocks to industries. Where needed, the intermittent nature of renewable energy generation can be addressed by using hydrogen storage to ensure continuous feedstock and energy supply to maintain the steady-state operation of industrial processes. Such systems can be used for diverse applications beyond steel and ammonia.

1.2 Hybrid Systems

A hybrid energy system is any energy system consisting of multiple generation and/or storage technologies. Batteries, heat, hydrogen storage, and other storage mediums can help reduce the variability inherent in many renewable energy sources such as wind and solar. Using multiple complementary energy generation technologies can also reduce the variability of the power available from hybrid renewable energy plants (Harrison-Atlas et al. 2022). Because energy storage can be costly (U.S. Department of Energy 2024), especially enough storage to provide for a steady load from renewable energy sources, reducing the variability of the sources can be an important step in industrial processes that require a stable energy source.

One approach to applying hybrid energy plants to heavy industry is to build dedicated energy systems for a given industrial process on the consumer side, or “behind the meter.” In the case of such behind-the-meter plants, which may not be connected to the grid, reducing the variability becomes even more critical for many reasons, such as to maintain more steady production, to avoid curtailing or losing generated electricity, and to reduce costs by reducing storage requirements. Behind-the-meter hybrid systems may also have other advantages in that they can be designed specifically for the designated use, they can potentially take advantage of intermediate storage capabilities beyond batteries (e.g., hydrogen), they do not rely on interconnection or grid updates, and they can pass all cost savings on to the operators of the end-use production plant.

1.3 The Role of Reference Designs, Use Cases, and Examples

Hybrid renewable systems for industrial energy are challenging to design and build. Each of the subsystems is itself a complex system requiring substantial modeling and design effort. There is a strong history of reference designs in wind energy (Gaertner et al. 2020; Jonkman 2009; Zaijjer et al. 2024) and other fields. For example, wind turbine reference designs are used by both academia and industry for a wide range of research and development efforts.

We seek to build on that tradition to encourage similar progress in hybrid renewable energy systems for industrial energy. In order to facilitate comparative research and development, we have developed this set of reference designs. The intent is that these reference designs will serve as a common baseline for researchers and as a starting point for industry stakeholders integrating renewables and other energy sources into their industrial processes.

1.4 Model Availability

The reference design files are freely available on GitHub at <https://github.com/NREL/ReferenceHybridSystemDesigns>. The modeling software, Green Hydrogen Energy and Renewable Technology (GreenHEART), used in the development of the reference designs is also available as open-source code on GitHub at <https://github.com/NREL/GreenHEART>. Questions, comments, or contributions can be made through the GitHub repositories.

2 Reference Design Development

In developing the reference designs, we aimed to represent a range of different environments. The reference designs were developed with input from multiple national laboratories and an industrial advisory board. We tried to include as much detail as is reasonable, but these reference designs are not intended to be ready-to-build designs. The designs represent both onshore and offshore subsystems and three products: hydrogen, ammonia, and steel.

We chose hydrogen because it can be used in a wide range of applications such as chemical manufacturing, steel-making, energy storage, and transportation.

The steel and ammonia cases were chosen as fully onshore systems. We selected hydrogen as the end product for the systems using offshore wind.

2.1 Onshore Systems

Two of the three reference designs have generation and production systems located onshore and are designed through an end product. Because hydrogen is used in many industrial processes, these plants are representative of how vertically integrated systems—from renewable generation to end product—could work. Each of the reference designs with only onshore components follow the general flow diagram shown in Figure 4.

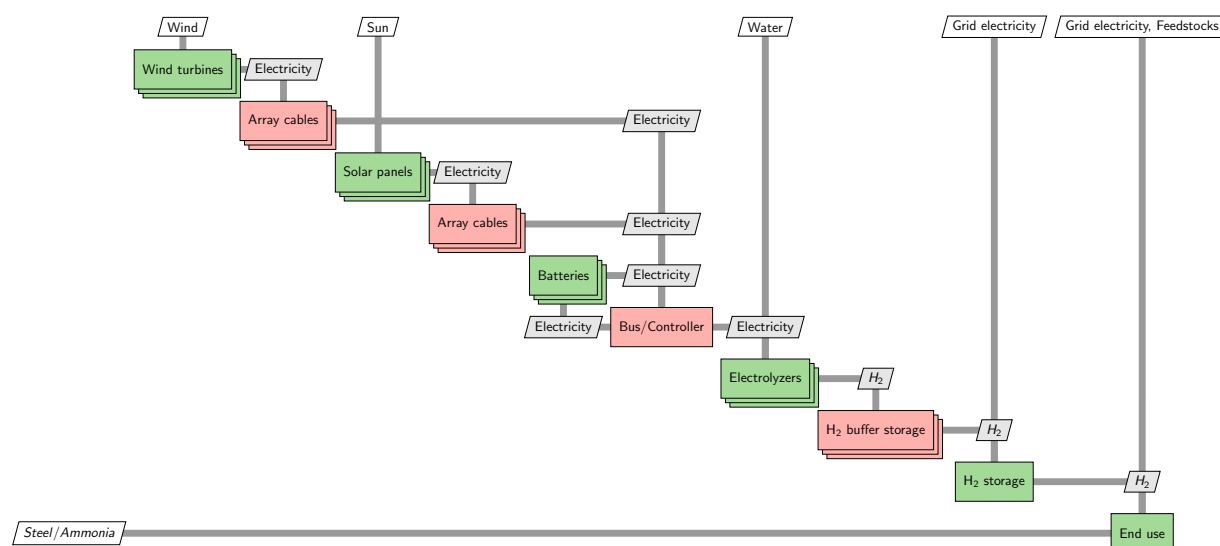
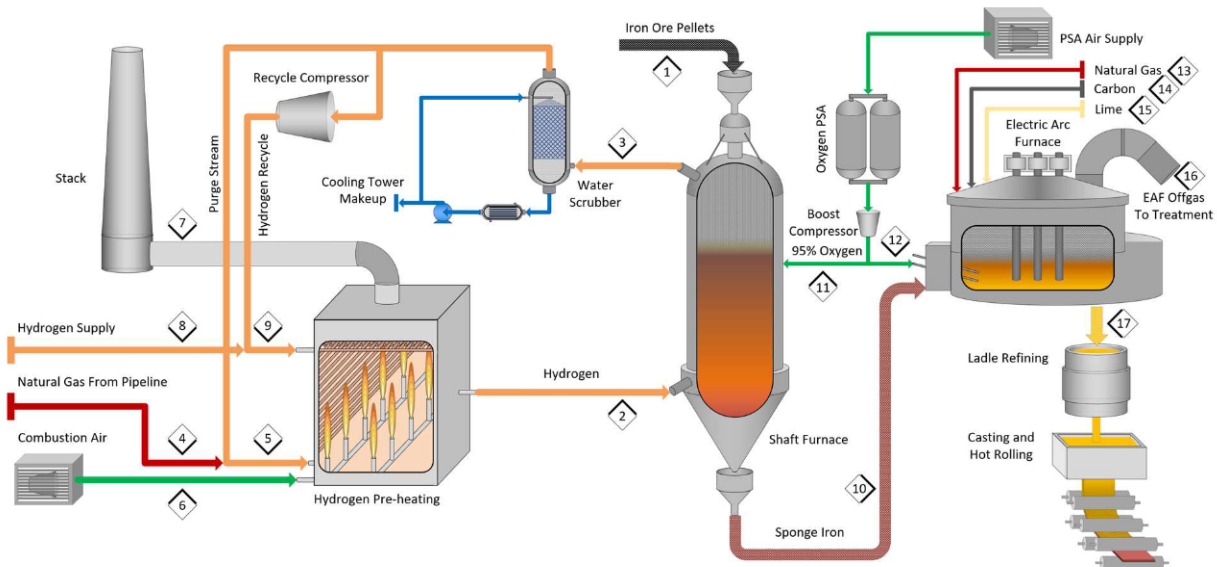


Figure 1. Onshore system eXtended Design Structure Matrix (XDSM) diagram (see Lambe and Martins 2012 for information about XDSM diagrams). Green indicates onshore systems, red indicates systems that are not explicitly modeled, stacks represent multiples of the component, gray/white boxes to the side of colored boxes indicate outputs, gray/white boxes above or below colored boxes indicate inputs.

The United States produced almost 95 million metric tons of steel in 2022. Blast furnaces produce approximately 30% of this steel, and electric arc furnace (EAF) produce the other 70% using a combination of scrap (90%) and high-quality raw material (10%) in the direct reduction iron (DRI)-EAF process (American Iron and Steel Institute 2023; Terry et al. 2023). All current steel production routes are emission-intensive, including most existing DRI-EAF steelmaking. Further, DRI-EAF currently has one of the highest technology readiness levels compared to alternative steelmaking technologies; therefore, it was selected for the reference designs. For more information on green steel production, see Reznicek et al. (2024).

Ammonia is used widely in the chemical industry. Its primary application is as a fertilizer, and it is also involved in the manufacturing of plastics, textiles, dyes, and explosives, among other products. In the United States, ammonia production in 2022 was 13 million metric tons (Statista 2023). Ammonia is produced by reacting hydrogen and nitrogen in the Haber-Bosch process (see Figure 3). As a product of hydrogen, ammonia can also be valuable as



a hydrogen or energy carrier because of the existing expertise in ammonia transportation, handling, and storage (Decarbonization Technology 2023; U.S. Department of Energy 2006).

2.2 Offshore Systems

baseline designs that indicate how such offshore development may benefit and be incorporated into hybrid energy systems.

All three reference designs with an offshore component have hydrogen gas as their end product. This decision was made because hydrogen is a precursor to many other products, so these plants could be extended to other products. Each of the reference designs with offshore components follows the general flow diagram shown in Figure 4.

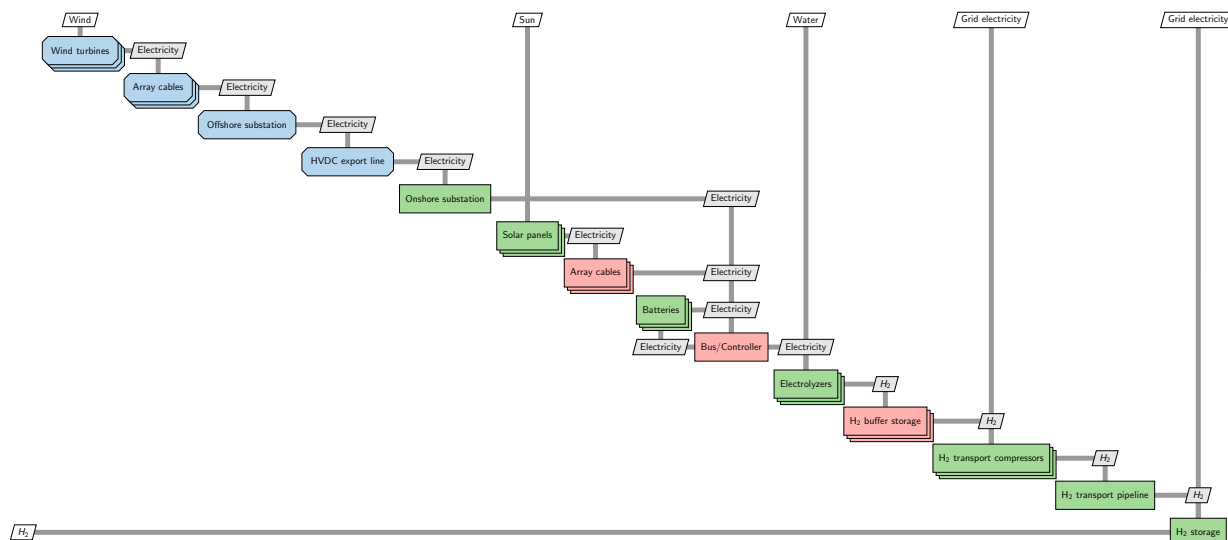


Figure 4. Offshore system XDSM diagram (Lambe and Martins 2012). Blue indicates offshore, green indicates onshore, red indicates not explicitly modeled, stacks represent multiples of the component, gray/white boxes to the side of colored boxes indicate outputs, gray/white boxes above or below colored boxes indicate inputs.

2.3 Site Selection

The sites were selected based on regional characteristics as well as economic considerations. Minnesota was selected as a reference location because it has adequate wind (see Figure 5) and solar (see Figure 6) resources and easy access to critical material feedstocks for steel production, including water and iron ore. The region also has the potential for geologic hydrogen storage in the form of hard rock cavern storage (see Figure 7). Texas was chosen based on its strong wind resource and access to geologic salt caverns for hydrogen storage. Three offshore wind locations were selected: New York Bight, the Gulf of Mexico, and California. All three locations were selected in areas with the strongest wind resource off each coast. The New York Bight site is near areas that are actively being leased and developed for fixed-bottom offshore wind energy. It is located near hard rock cavern storage onshore. The Gulf of Mexico site was selected because of its access to existing hydrogen infrastructure and salt cavern storage and potential for development as a fixed-bottom offshore wind location. The California site was selected as a representative floating offshore wind location to demonstrate the differences between fixed and floating offshore wind locations.

2.4 Design Tools and Methods

We used the GreenHEART software (National Renewable Energy Laboratory 2025a) to model and design the reference plant systems. GreenHEART uses the Hybrid Optimization and Performance Platform (HOPP) software (Tripp et al. 2019) to model the electrical generation and dispatching for hybrid energy plants. The HOPP model used the Python package of the System Advisor Model (PySAM) version 4.2.0 to access PVWatts@Version 8 PV solar model for the solar technology (National Renewable Energy Laboratory 2023). Our HOPP model used the FLOW Redirection and Induction in Steady state (FLORIS) software (Gebraad et al. 2014) for modeling the flow physics in the wind farm. The battery dispatch model is a reduced-order representation of the battery in HOPP, which tells the PySAM battery model (National Renewable Energy Laboratory 2023) how to dispatch to meet the desired load. GreenHEART uses the Offshore Renewables Balance-of-System and Installation Tool (ORBIT) (Nunemaker et al. 2020) for the offshore wind farm costs and internal models for hydrogen production, hydrogen storage, ammonia production, and steel manufacturing. GreenHEART then connects the HOPP outputs with outputs from the other models and uses ProFAST (Kee and Penev 2023) to do a cash flow financial analysis for the life of the hybrid plant.

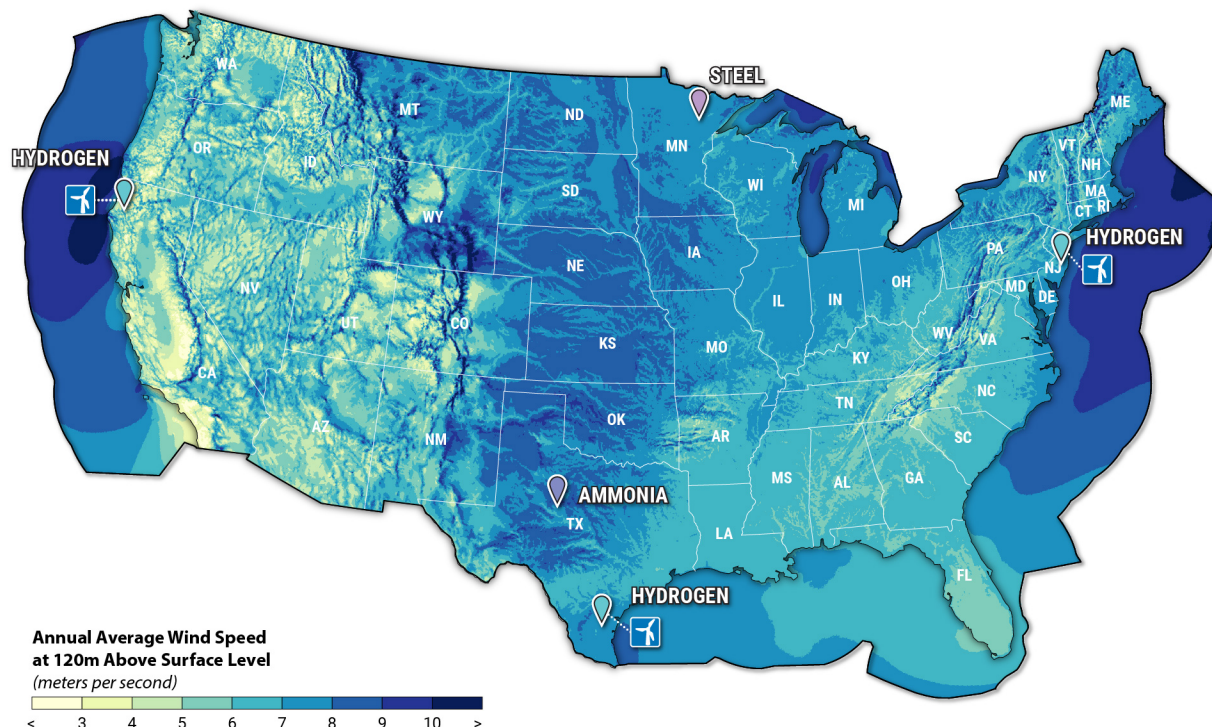


Figure 5. Wind resource map for the contiguous United States, including reference design locations. Locations shown are approximate. Dashed lines and wind turbine icons indicate systems with separate locations for the wind turbines and the remaining plant elements. Map illustration by Billy Roberts, NREL.

2.5 Design Space Exploration

We used the subsystem sizes from Reznicek et al. (2024) as a starting point. Keeping the wind plant rating constant, we ran coarse sweeps of the design space by taking uniformly spaced samples for all combinations of the other subsystem ratings in a full-factorial approach. We then down-sampled the results to get the samples with the lowest levelized cost of product. While the lowest-cost designs showed little to no battery storage, operating such plants without any battery storage for black starts and ancillary power is not reasonable. For this reason we selected plants that still had some battery storage but also fell in the low-cost data. We then used the Sparse Nonlinear OPTimizer (SNOPT) to further refine the plant sizing from the selected points by minimizing the objective function with respect to the PV capacity, battery energy and power, and electrolyzer capacity, where the objective could be the levelized cost of steel (Reference Design 01), the levelized cost of ammonia (Reference Design 02), or the levelized cost of hydrogen (Reference Designs 03–05).

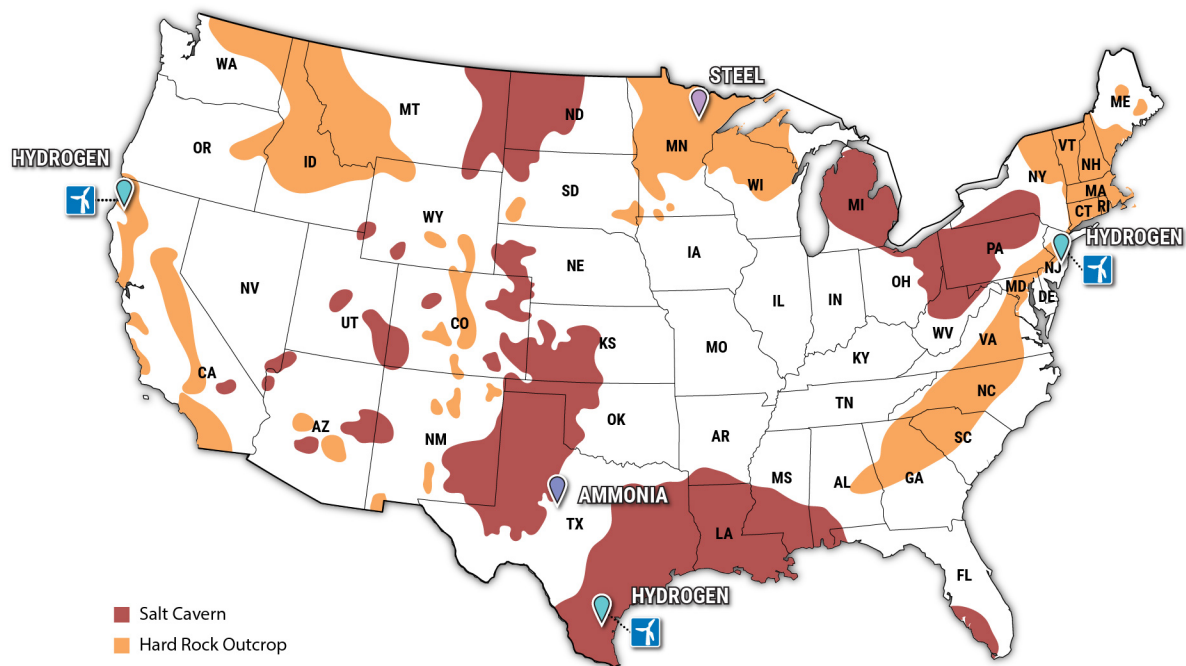


Figure 7. Geologic storage resource map for the contiguous United States, including reference design locations. Locations shown are approximate. Dashed lines and wind turbine icons indicate systems with separate locations for the wind turbines and the remaining plant elements. Map illustration by Billy Roberts, NREL.

3 Reference System Designs

This section provides the technical details of the reference designs, including costs, subsystem sizing and connections, and details about the design and components of the subsystems. This section also addresses production expectations and safety. Section 3.1 provides detailed information for components and subsystems that are shared across multiple systems and details that are easier to present in a common location than dispersed through documentation on the individual subsystem sections. Section 3.2 provides the general system design information and a high-level comparison between the designs. Individual reference design information is presented in Section 3.3 through Section 3.7.

3.1 Common Subsystem Assumptions and Designs

This section provides details that pertain to multiple reference designs to avoid duplication of information. The site-specific sections refer back to this section for details as appropriate. In some cases the information in this section is only relevant to a single site but is included here to be near similar information for easy reference. It is important to note that there are significant differences in the level of detail included for the onshore systems as compared to the offshore systems. This is in part due to model availability and different capabilities available in the software for the onshore systems versus the offshore systems.

3.1.1 Wind

Common and comparable information are presented here for the wind farm subsystem in each of the reference designs. The modeling for the offshore wind farms was done using the ORBIT software for offshore balance of station design and costs (Nunemaker et al. 2020) from the National Renewable Energy Laboratory (NREL) as well as an NREL's nationwide analysis of offshore wind costs (Fuchs et al. 2024), so it contains a high level of detail. However, GreenHEART does not currently include any models with a comparable level of detail for balance of system costs for onshore wind farms. Wind turbine design, performance, and cost all have similar levels of detail across all reference design locations.

The onshore reference designs use the 6-MW 2024 Annual Technology Baseline (ATB) wind turbine (Eberle et al. 2024), whereas the offshore reference designs use either the International Energy Agency Wind Technology Collaboration Programme 15-MW reference turbine Gaertner et al. 2020 or the 17-MW low-specific-power turbine (Fuchs et al. 2023). The wind turbines' thrust and power curves are provided in Figure 8. Other details of the wind turbines are provided in Table 1.

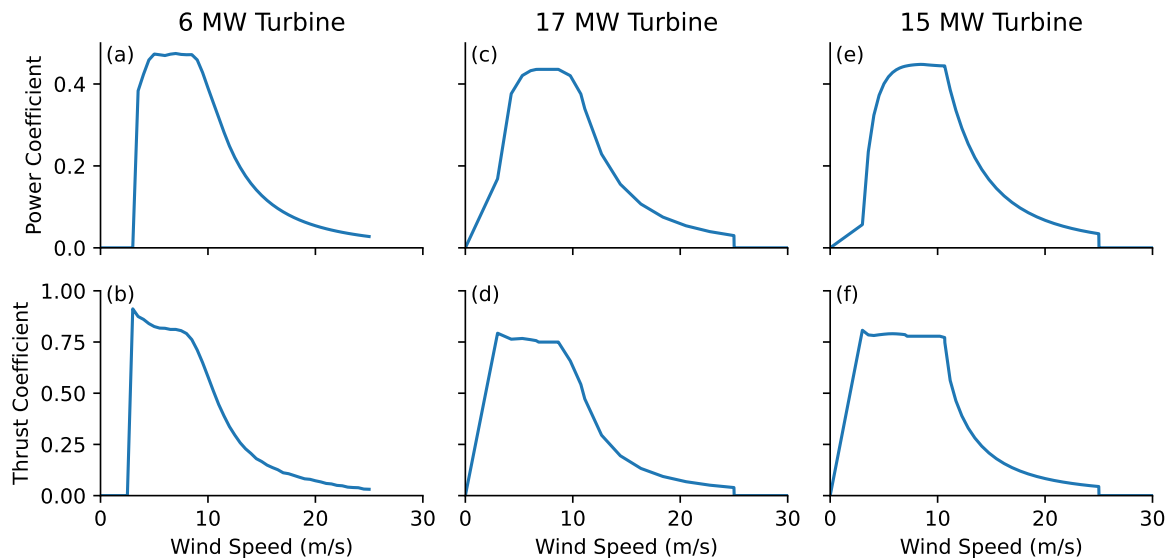


Figure 8. Wind turbine performance curves

Table 1. High-level wind turbine design specifications

Turbine Rating (MW)	6	15	17
Rotor diameter (m)	170	242.24	278.035
Hub height (m)	115	150	168
Tilt (deg.)	6	6	6
Rated wind speed	11	10.66	7
Tip-speed ratio	9	9	9

The onshore wind farm balance of system is in terms of losses and costs. The operational loss for the onshore wind farms is assumed to be 10.49% based on the PySAM default and adjusted losses shown in Table 2 (National Renewable Energy Laboratory 2023). The balance of system costs are assumed to be included in the per-kilowatt inputs for each technology based on the 2024 ATB (National Renewable Energy Laboratory 2024). Cable types and layout are not defined. Because the onshore systems are assumed to be fully co-located with the rest of the hybrid systems, they do not need substations or export cables as required by the offshore wind farms.

Table 2. Wind balance of plant power losses. While HOPP excludes the turbine operational and wake losses by default when using FLORIS as the wake model (for a total wind balance of plant loss of 12.83%), the reference designs additionally exclude the grid availability and the grid curtailment losses because the plants are assumed to be grid disconnected.

Loss Type	Power Loss (%)	
	PySAM Default	Reference Designs
Balance of plant availability loss	0.5	0.5
Grid availability loss	1.5	0.0
Turbine availability loss	3.58	3.58
Electrical efficiency loss	1.91	1.91
Electrical parasitic consumption loss	0.1	0.1
Environmental degradation loss	1.8	1.8
Environmental external conditions loss	0.4	0.4
Environmental exposure loss	0.0	0.0
Environmental icing loss	0.21	0.21
Environmental/permit curtailment loss	1.0	1.0
Grid curtailment loss	0.84	0.0
Load curtailment loss	0.99	0.99
Operational strategies loss	0.0	0.0
Turbine generic power curve loss	1.7	0.0
Turbine high wind hysteresis loss	0.4	0.0
Turbine suboptimal performance loss	1.1	0.0
Turbine site-specific power curve loss	0.81	0.0
External wake loss	1.1	0.0
Total	17.94	10.49

Table 3 shows the assumptions and specifications for the offshore electrical cables. The individual turbines are connected to the offshore substation through strings of array cables rather than being connected individually. The electrical properties described in Table 3 determine how many turbines can be linked to a single string. Cable costs are modeled based on the cost per kilometer. The model assumes that the array cable system transmits balanced three-phase AC power.

The number of substations depends on the high-voltage direct current (HVDC) or high-voltage alternating current (HVAC) export cables. At a minimum there is one offshore substation and one onshore substation. For the offshore substation the design and costs are based on the required equipment on the substation's topside. The equipment in Table 4 is included in the offshore substation design for each specific cable type. The overall output relating to the offshore substation is the mass of the topside and substructure and associated costs.

Table 3. Offshore Cable Specifications

	Array Cables				Export Cables		
	A1	A2	A3	A4	E1	E2	E3
AC resistance (ohm/km)	0.128	0.04	0.128	0.04	0.16	N/A	0.16
Capacitance (nF/km)	163	300	163	300	190	N/A	190
Conductor size (mm ²)	185	630	185	630	1000	2000	1000
Cost (USD/km)	200,000	400,000	240,000	480,000	850,000	500,000	1,020,000
Current capacity* (A)	445	775	445	775	825	1,900	825
Inductance (mH/km)	0.443	0.35	0.443	0.35	0.38	0.127	0.38
linear density (t/km)	26.1	42.5	26.1	42.5	115	53	115
Coating	XLPE	XLPE	XLPE	XLPE	XLPE		XLPE
Rated voltage (kV)	66	66	66	66	220	320	220
Switchgear cost (USD)		1,000,000		1,000,000			
Current type	HVAC	HVAC	HVAC	HVAC	HVAC	HVDC**	HVAC
Dynamic	No	No	Yes	Yes	No	No	Yes

* at 2-m burial depth

** monopole

Table 4. Equipment Included on Offshore Substation for HVAC and HVDC Export

Equipment	HVAC	HVDC
Main power transformer	Yes	No
Shunt reactor	Yes	No
Switch gear	Yes	No
Converter	No	Yes
DC breaker	No	Yes
Ancillary system	Yes	Yes

The onshore substation includes an onshore converter (for HVDC), switchgear (for HVAC), main power transformer (for HVAC), and shunt unit (for both). Sites utilizing fixed-bottom technology adopt a default monopile substructure design from ORBIT (Nunemaker et al. 2020). The monopile's dimensions—diameter, thickness, and length—are scaled according to turbine specifications (rotor diameter and hub height) and site conditions (water depth).

Scour protection made up of rock, sand, or other similar material is included at the base of the monopile. The design includes a cost per metric ton of material and the depth of scour protection. Additional scour options are available in ORBIT, but the defaults were used for the reference designs.

The transition piece design is based on the resultant monopile design. The transition piece is composed of steel and assumed to be 25 m in length.

In locations utilizing fixed-bottom technology, the array cables were assumed to be installed under the seabed using an installation vessel that simultaneously lays and buries the cable along the route from the offshore substation to each turbine along the string.

Offshore substations in fixed-bottom locations use a monopile substructure design, which is assumed to be 40% the mass of the topside mass. The substructure costs are composed of primary substructure material and pile material costs.

The sites utilizing floating technology use a semisubmersible substructure design composed of three stiffened columns with attached heave plates to provide turbine stability linked together via a truss (Maness, Maples, and Smith 2017). The substructures are attached to the seabed via a mooring and anchor system. The anchor system is a drag embedment with a default 500 m of additional mooring line length. The mooring line length and mass is determined based on the site's seabed depth and rope and chain modeling by MoorPy (Hall et al. 2021).

3.1.2 Solar PV

The solar PV plant is modeled using the PVWatts Version 8 module available in PySAM National Renewable Energy Laboratory 2023. The design of the PV system is aligned with the representative technology presented in NREL's 2024 ATB. The PV system comprises one-axis tracking standard monofacial modules with a 45° rotational limit, DC-to-AC ratio of 1.34, 96% inverter efficiency, and 14.0757% DC losses.

The PV system is south-facing and has a ground coverage ratio of 0.3. The tilt angle of the panels, θ , is calculated based on the site's latitude, lat , as given by Eq. 3.1:

$$\theta = \begin{cases} 0.87lat & \text{if } lat \leq 25 \\ (0.76lat) + 3.1 & \text{if } 25 < lat \leq 50 \\ lat & \text{if } lat > 50 \end{cases} \quad (3.1)$$

The PV system mass and footprint are estimated with respect to the reference module described in Table 5. The

Table 5. Reference PV Module Design Specifications

Rated Power	Width	Length	Area	Unit Mass
321 Wdc	1.488 m	0.992 m	11.904 m ²	11.092 kg/m ²

number of modules within the PV system, $N_{modules}$, is calculated as:

$$N_{modules} = \frac{P_{system}}{P_{ref}} \quad (3.2)$$

where P_{system} is the DC capacity of the PV system and P_{ref} is the DC capacity of the reference module given in Table 5. The PV system area, A_{system} , is calculated as:

$$A_{system} = A_{module} N_{modules} \quad (3.3)$$

where A_{module} is the module area given in Table 5. The PV system mass, m_{system} , is then calculated as:

$$m_{system} = A_{system} m_{module} \quad (3.4)$$

where m_{module} is the reference module unit mass given in Table 5.

System costs were obtained from NREL's 2024 ATB for utility-scale PV with a technology year of 2030 and the Moderate technology advancement scenario (National Renewable Energy Laboratory 2024). The ATB system costs are provided in \$/kW_{AC} and converted to \$/kW_{DC} using a DC-to-AC ratio of 1.34, as given in Table 6.

Table 6. 2030 Utility-Scale PV System Costs in 2022 USD

	Overnight Capital Cost	Fixed Operations & Maintenance Cost
DC-rated	779.1 \$/kW _{DC}	13.43 \$/kW _{DC} -year
AC-rated	1,044 \$/kW _{AC}	18 \$/kW _{AC}

3.1.3 Battery Storage

The battery is a lithium-ion lithium-iron-phosphate (LFP/graphite) battery, with properties given in Table 7 and 8.

HOPP currently uses PySAM for the simulation of battery storage technologies (Danecek et al. 2021). In HOPP, the battery's operation is governed by the following equation, where τ represents the look-ahead time period and t represents a time index. These dynamics are detailed in W. Hamilton et al. (2022) and are summarized here.

$$b_t^{soc} = b_{t-1}^{soc} + \Delta \left(\frac{\eta^+ \cdot \dot{w}_t^+ - \dot{w}_t^- / \eta^-}{CB} \right) \quad \forall t \in \tau : t \geq 2 \quad (3.5)$$

Equation 3.5 represents the update to the battery state of charge, b_t^{soc} , and is dependent on the previous state of charge; the time step, Δ ; the charge efficiency, η^+ ; the discharge efficiency, η^- ; the power in and out of the battery at

Table 7. Parameters of the battery in the PySAM battery model.

Parameter	Value
Rate of voltage vs. capacity curve input	0.2
Cell capacity at end of exponential zone [Ah]	0.04
Fully charged cell capacity [Ah]	2.25
Cell capacity at end of nominal zone [Ah]	2.0
Cell voltage at end of exponential zone [V]	4.05
Fully charged cell voltage [V]	4.1
Cell voltage at end of nominal zone [V]	3.4
Default nominal cell voltage [V]	3.6
Cell cutoff voltage [V]	2.706
Internal resistance [Ohm]	0.002
Battery specific heat capacity [J/kgK]	1500.0
Temperature of storage room [°C]	20
Table with temperature and capacity	see Table 8
Heat transfer between battery and environment [W/m ² K]	7.5
Battery mass per string [kg]	152.227
Nominal installed energy [kWh]	10.0
Nominal DC voltage [V]	500.0
Battery total surface area per cell [m ²]	1.53934

Table 8. Capacity vs. temperature for the PySAM battery model.

Temperature (°C)	Capacity (%)
-20	72.33
-10	81.8
0	88.8
10	93
23	96.67
45	101
60	101

time t , which is \dot{w}_t^+ and \dot{w}_t^- , respectively; and the battery manufactured specified capacity, C^B . The state of charge is bounded by the equation $\underline{S}^B \leq b_t^{soc} \leq \bar{S}^B, \forall t \in \tau$, where \underline{S}^B and \bar{S}^B are the minimum and maximum operation bounds of the battery state of charge, respectively.

The power flow in and out of the battery is also bound by constraints that have the following form:

$$\underline{P}^B y_t^- \leq \dot{w}_t^- \leq \bar{P}^B y_t^- \quad (3.6)$$

$$\underline{P}^B y_t^+ \leq \dot{w}_t^+ \leq \bar{P}^B y_t^+ \quad (3.7)$$

where \underline{P}^B and \bar{P}^B are the battery minimum and maximum power ratings, respectively, and y_t^- and y_t^+ are indicators of whether the battery is charging or discharging during time period t . These indicators have a value of 1 if the battery is discharging (y_t^-) or charging (y_t^+) during the time period, and 0 otherwise. The indicators are also subject to the constraint $y_t^+ + y_t^- = 1$ to ensure the battery is only performing one activity over each time period. Finally, the cycle count of the battery is calculated using

$$b^c \geq \frac{\Delta}{C^B} \sum_{t \in \tau} \dot{w}_t^- \quad (3.8)$$

Bounds on some of the variables are enforced subject to the following constraints:

$$b^c, b_t^{soc}, \dot{w}_t^+, \dot{w}_t^- \geq 0 \quad \forall t \in \tau \quad (3.9)$$

$$y_t^+, y_t^- \in \{0, 1\} \quad \forall t \in \tau \quad (3.10)$$

The dispatch of hybrid systems is more complex than that of single-technology variable renewable energy generators, as it requires the coordination of all the included technologies. In HOPP, this coordination is accomplished by implementing a modular framework where each technology operates as a separate module (W. Hamilton et al. 2022). More information on this structure and the dispatch of the systems, such as the grid system and the photovoltaic system, is available in W. Hamilton et al. (2022) and W. T. Hamilton et al. (2020). Here, we focus only on the battery dispatch in a load-following scenario.

The dispatch strategy for the battery focuses on meeting load demand without considering cost. The battery dispatch uses a simplified heuristic method, making decisions to meet the load demand signal at each time step and without accounting for future information. The logic starts by taking the difference between the overall generated power and the load requirement as $\Delta w_t = (W_t^g - \dot{w}_t^{hybrid})$, borrowing W_t^g as the load requirement from the previous section, \dot{w}_t^{hybrid} as the total hybrid power production, and Δw_t as the power difference, all at time t . The change in the power from the battery is then decided according to:

$$\dot{w}_t = \begin{cases} -\min(|\Delta w_t|, \Delta \dot{C}^-) & \text{if } \Delta w_t < 0 \\ \min(|\Delta w_t|, \Delta \dot{C}^+) & \text{if } \Delta w_t > 0 \\ 0 & \text{otherwise} \end{cases} \quad (3.11)$$

where \dot{C}^- and \dot{C}^+ are the discharge and charge rates of the battery, respectively. If the generation is equal to the load, then the battery does nothing.

The state of charge is updated according to the following equations:

$$b_t^{soc} = \begin{cases} \min[(b_{t-1}^{soc} + \dot{w}_t), \underline{S}^B] & \text{if } \Delta w_t < 0 \\ \max[(b_{t-1}^{soc} + \dot{w}_t), \bar{S}^B] & \text{if } \Delta w_t > 0 \\ b_{t-1}^{soc} & \text{otherwise} \end{cases} \quad (3.12)$$

where b_{t-1}^{soc} represents the state of charge at the previous time step. This logic also enforces the bounds on the state of charge of the battery: $\underline{S}^B \leq b_t^{soc} \leq \bar{S}^B, \forall t \in \tau$. Because this method is a faster heuristic method, it operates without minimizing the operating costs and only considers meeting the load profile for the system.

In this analysis, the logic outlined in the previous paragraph is meant to require a minimum output from the plant. The maximum output of the plant is capped at the interconnection (or capacity) of the plant.

3.1.4 Electrolysis PEM

The proton exchange membrane (PEM) electrolyzer system comprises multiple *clusters*. Each cluster is made up of multiple series-connected 1-MW stacks. Clusters can be operated independently of each other. The cluster has a maximum rating of 40 MW based on current rectifier technology. Primary details of the electrolyzer model are provided in Table 9. A cluster is replaced when it reaches end of life (EOL). EOL is defined as a 13% efficiency

Table 9. 1-MW PEM Electrolyzer Model Parameters

Parameter	Variable	Value	Units
Number of cells/stack	n_{cells}	130	[-]
Cell membrane thickness	$\delta_{membrane}$	0.018	cm
Cell active area	A_{cell}	1,920	cm ²
Operating temperature	T_{op}	353.15	K
Rated current density	J_{max}	2	A/cm ²
Stack rated power	P_{rated}	1,000	kW
Turndown ratio	TR	10	% Load
rated conversion efficiency	$\eta_{max,BOL}$	54.6	kWh/kg

drop, measured at rated, from beginning of life (BOL). The cluster has a maximum stack life of 77,600 hours. The cluster replacement cost is assumed to be 15% of the overnight capital cost of the cluster.

The electrolyzer model uses a simple equal-power-split dispatch strategy to divide up the available power among the clusters.

3.1.5 Hydrogen Storage

There are two types of geologic storage considered for hydrogen in the reference designs: salt caverns and hard rock caverns (or lined-rock caverns). Salt caverns have already been demonstrated for hydrogen storage, while hard rock caverns, though not proven at the industrial scale, have been used in pilot projects for natural gas storage. The geologic storage models draw from Papadiaz and Ahluwalia (2021) for capital costs and the Hydrogen Deliver Scenario Analysis Model (HDSAM) Version 4.0 Gaseous H₂ Geologic Storage (Argonne National Laboratory 2023) for operational costs. It is assumed in the design that the necessary geologic surveys have confirmed the suitability of potential salt and hard rock caverns, as shown in Figure 7, for hydrogen storage development. The salt caverns are created from existing natural salt beds, with capital costs covering new cavern construction, aboveground facilities, brine transport, and brine disposal (Papadiaz and Ahluwalia 2021). Hard rock caverns, made of low-permeability rock with minimal fissures, can be fitted with liners—either polymer membranes or thin steel sheets—to minimize hydrogen leakage. The main capital costs for hard rock caverns include tunnel and cavern excavation, drainage, liner and concrete installation, and aboveground facilities. The installed hydrogen storage capital costs are represented in Equation (3.13) (Papadiaz and Ahluwalia 2021), with coefficient values shown in Table 10 (Papadiaz and Ahluwalia 2021).

$$\text{Installed capital cost} = \exp(a(\ln(m)))^2 - b\ln(m) + c \quad (3.13)$$

Table 10. Coefficients for installed capital costs for hydrogen storage (adapted from Papadiaz and Ahluwalia (2021))

Storage	a	b	c
Lined hard rock caverns	0.095803	1.5868	10.332
Salt caverns	0.092548	1.6432	10.161

The design assumes that the hydrogen is transported to the geologic storage via a pipeline and discharges to a pipeline. There are a minimum of two equally sized compressors for operation; the compressors are based on the hydrogen compressor from HDSAM Version 3.1 (*Hydrogen Delivery Scenario Analysis Model*,). One compressor takes the hydrogen and compresses it into the geologic storage (120 bar for salt cavern storage and 200 bar for hard rock storage), and the other takes the hydrogen from the geologic storage and compresses it into the pipeline for use. The compressors have a maximum motor rating of 16,000 kW, and if the required power is greater than the maximum, another compressor is added to ensure the compressors are able to handle the total hydrogen throughput.

The hydrogen storage is sized to provide steady-state delivery of hydrogen from the storage. The assumed hydrogen demand is the average of the hourly hydrogen production from the electrolyzer. The state-of-charge of the hydrogen storage is then tracked as the absolute mass of hydrogen stored. The hydrogen stored or discharged is based on the difference between the hourly hydrogen production rate and the average demand. It is assumed that the storage is able to fully charge and discharge, and the required head capacity is not calculated.

3.1.6 Ammonia

Table 11 provides cost factors for ammonia plants. The reported data have been collected by previously conducted work (Lee et al. 2022). The cost factors can be used with the following equation to determine each components cost:

$$C_i = \alpha_i S_i^{\beta_i} \quad (3.14)$$

where α_i and β_i are the respective constant and scale factors associated with a plant component i , and S_i is the capacity or size of a component. The total capital cost is a summation of the plant's components' capital costs.

Table 11. Ammonia Cost Coefficients (Lee et al. 2022)

Ammonia Plant Component	Constant α	Scale Factor β
Haber-Bosch loop	18,642,800	0.6
Air separation (cryogenic distillation)	22,506,100	0.6
Boiler and steam turbine	7,069,100	0.6
Cooling tower	4,799,200	0.6
Depreciable non-equipment	4,112,702	0.6
Land	2,500,000	1
Labor cost	5,928,000	0.25
Maintenance cost	0.5% of total capital expenditures	0.6

Table 12 provides the ammonia plant consumption rates for different feedstocks as well as the cost of the iron-based catalysts the plant requires. The consumption rates are based on the specific technology and flowsheet presented in Figure 3. Hydrogen, grid electricity, and cooling water costs all vary by location, as detailed subsequently; this work assumes a constant iron-based catalyst cost across all selected sites for analysis. The feedstock cost is the product of the consumption rate and unit cost of each feedstock.

Table 12. Ammonia Plant Feedstock Consumption and Cost per Kilogram of Ammonia (Lee et al. 2022)

Feedstock	Consumption	Units	Cost (\$2020/unit)
Hydrogen	0.19728	kg	location-dependent
Electricity	0.12073	kWh	location-dependent
Cooling water	0.04924	gallon	location-dependent
Iron-based catalyst	9.130×10^{-5}	kg	23.19977341

3.1.7 Steel

Table 13 gives the capital cost coefficients for different steel plant components. The values have been taken from a variation of the model published in Rosner et al. (2023b). These coefficients should be used with Eq. 3.14.

Table 14 gives steel plant feedstock and byproduct consumption/production and cost. The presented costs count toward variable operating costs and depend on the plant's operation scheduling. Iron ore, raw water, lime, carbon, hydrogen, and electricity are all consumed in the process; hence, their annual usage will depend on the capacity factor of the steel facility.

3.1.8 Reference Design Costs

The grid is used to power the ammonia and steel plants. Table 15 gives the assumed grid electricity retail prices for each location over time for a mid-cost scenario. The cost of grid electricity for years in between those shown in the table is interpolated. It is also assumed the costs remain constant after year 2050. In the analysis, it is assumed that in each year, each end-use plant uses the same amount of grid electricity each year.

Table 13. Steel Plant Cost Coefficients (Rosner et al. 2023b)

Steel Plant Component	Constant α	Scale factor β
EAF and casting	352,192	0.46
Shaft furnace	490	0.89
Oxygen supply	1,715	0.65
Hydrogen preheating	46	0.86
Cooling tower	2,513	0.63
Piping	11,816	0.59
Electrical & instrumentation	7,877	0.59
Buildings, storage, water service	1,098	0.80
Other miscellaneous costs	7,877	0.59
Labor cost	2,042,784	0.252

Table 14. Steel Plant Feedstock/Byproduct Consumption/Production per metric ton of Steel (Rosner et al. 2023b)

Feedstock	Consumption	Units	Cost (2022 USD/unit)
Iron ore (DRI-grade pellet, 66% Fe)	1.6293	metric tons	224
Raw water	0.8037	metric tons	0.64
Lime	0.0181	metric tons	108
Carbon	0.0538	metric tons	205
Maintenance materials	1	metric tons	8.34
Hydrogen	0.0660	metric tons	location-specific
Natural gas	0.7166	GJ-LHV	location-specific
Electricity	0.5502	MWh	location-specific
Byproduct	Production	Units	Disposal Cost (2022 USD/unit)
Slag	0.1743	metric tons	41
Surface water discharge	0.4211	metric tons	-

We used a medium retail grid price scenario for our analysis. We estimated the retail prices for the mid-case scenario using the following steps:

1. Obtain the annual average retail prices for 2022 from the U.S. Energy Information Administration Annual Energy Outlook 2022 (EIA 2023) for each region of interest.
2. Calculate the average annual wholesale rates for each region of interest using NREL’s Cambium 2022 database “Mid-case 100% decarbonization by 2035” scenario.
3. Calculate the difference between the Annual Energy Outlook 2022 annual average retail rate and the Cambium average annual wholesale rate to obtain the regional wholesale markup.
4. Apply the regional 2022 wholesale rate markup to the average annual wholesale rate estimated by Cambium for each fifth subsequent analysis year (Cambium 2022 has a temporal resolution of 5 years) to get the estimated retail rate. This assumes that administrative and business costs that account for retail rate markup are constant over time.
5. Calculate a moving average rate for each year based on a weighted average. The weights assigned are 40% for the year in question and 30% each for the data 5 years prior and 5 years after the year in question.
6. Temporally interpolate the retail rates in each region to obtain the retail rates for the years not explicitly represented in Cambium.

Table 15 gives the resulting retail prices calculated for each year and each location. Also note the difference between technology year and commissioning year. Here, we assume that plants are brought online approximately 5 years later, and as a result, the first retail rate year occurs 5 years after a given technology year. We assume that each plant uses the same amount of grid electricity each year of its operation, with additional electricity allocated to account for electrolyzer cell stack degradation. We apply the changing grid prices throughout the plant’s life by interpolating the data in Table 15.

Table 15. Estimated annual average grid retail prices in 2022 USD/MWh based on methods discussed in Reznicek et al. (2024).

Year	Average Grid Retail Price (2022 USD/MWh)	
	Texas	Minnesota
2030	91	101
2035	106	101
2040	110	104
2045	98	91
2050	103	96

Table 16 gives the steel plant feedstock transportation costs for iron ore, lime, and carbon. Because iron ore mining is associated mainly with Minnesota, the transportation cost to the plant in that location is low. For more information on the transportation model, see Reznicek et al. (2024).

Table 16. Minnesota steel plant feedstock transportation costs (Transportation Statistics 2023).

Feedstock	Cost (2022 USD/metric ton)
Iron ore	0.63
Lime	47.72
Carbon	64.91

3.2 Reference Design Overview

An overview of the five reference designs is provided in Table 17. Presenting the size and specifications of each of the reference designs in one place is intended to make comparisons easier.

The financial assumptions used for each reference design are provided in Table 18. We have tried to make the financial assumptions reasonable for each location or region. Note that Texas does not have a state income tax but does have a franchise tax. We used the franchise tax rate in Texas in place of state income tax rate as an approximation of the franchise tax in Texas.

The cost assumptions for each technology are given in Table 19. Most of these costs come from the 2024 NREL ATB National Renewable Energy Laboratory 2024. However, some of the costs were determined during the simulation as functions of other inputs.

Table 17. Overview of Reference Designs

ID	01	02	03	04	05
State	Minnesota	Texas	Texas	New Jersey	California
Area			Gulf Coast	New York Bight	
Product	Steel	Ammonia	Hydrogen	Hydrogen	Hydrogen
On/Offshore	Onshore	Onshore	Offshore	Offshore	Offshore
Turbine foundation			Fixed	Fixed	Floating
Hydrogen storage type	Rock cavern	Salt cavern	Salt cavern	Rock cavern	Rock cavern
PEM electrolyzer rating (MW)	720.0	640.0	1,125.0	1,125.0	1,125.0
Wind farm rating (MW)	930.0	888.0	986.0	990.0	990.0
Solar PV rating (MW)	800.0	400.0	1,500.0	1,500.0	1,500.0
Total generation rating (MW)	1,730.0	1,288.0	2,486.0	2,490.0	2,490.0
Battery power rating (MW)	108.0	0.1	375.7	375.7	375.7
Battery energy rating (MWh)	108.0	0.1	1,500.0	1,500.0	1,500.0
Hydrogen generation rating (kt)	115.0	103.0	181.0	181.0	181.0
Hydrogen storage capacity (kt)	1.7	3.4	5.3	6.6	8.2
Hydrogen storage max fill rate (t/h)	13.2	11.7	20.7	20.7	20.7
Number of wind turbines	155	148	58	66	66
Wind turbine rating (MW)	6.0	6.0	17.0	15.0	15.0
Onshore latitude	47.5000	32.3171	27.6096	39.7755	40.8837
Onshore longitude	-93.0000	-100.1800	-97.4023	-74.2302	-124.1335
Offshore latitude			27.1808	39.5397	40.8538
Offshore longitude			-96.9330	-73.3299	-124.6752
Direct horizontal irradiance (kWh/m ²)	59.5	59.2	76.3	67.7	60.2
Average wind speed (m/s)	7.4	9.1	8.4	9.5	9.2
Steel capacity (Mt/yr)	1.0				
Ammonia capacity (kt/yr)		329.0			
LCOH (USD/kg-H ₂)	6.3	4.8	9.6	10.3	14.2
LCOS (USD/t steel)	1,191.0				
LCOA (USD/kg-NH ₃)		1.1			
Distance from shore (km)			44.7	71.1	40.9
Depth (m)			45.0	34.0	905.0

Table 18. Financial Assumptions

ID	01	02	03	04	05
State	Minnesota	Texas	Texas	New Jersey	California
Area			Gulf Coast	New York Bight	
Product	Steel	Ammonia	Hydrogen	Hydrogen	Hydrogen
Foundation			Fixed	Fixed	Floating
Real ROE wind (%)	6.30	6.30	7.00	7.00	7.80
Real ROE PV (%)	5.90	5.90	5.90	5.90	5.90
Real ROE battery (%)	6.60	6.60	6.60	6.60	6.60
Real ROE hydrogen (%)	10.20	10.20	10.20	10.20	10.20
Real ROE steel (%)	10.89				
Real ROE ammonia (%)		10.89			
Total income tax rate (%)	25.74	25.74	25.74	25.74	25.74
Capital gains tax rate (%)	15.00	15.00	15.00	15.00	15.00
Property tax rate (%)	2.00	1.47	1.47	2.08	0.68
Property insurance rate (%)	1.00	1.00	3.00	1.50	1.50
Debt percentage wind (%)	72.40	72.40	73.40	73.40	73.40
Debt percentage PV (%)	75.30	75.30	75.30	75.30	75.30
Debt percentage battery (%)	75.40	75.40	75.40	75.40	75.40
Debt percentage hydrogen (%)	38.50	38.50	38.50	38.50	38.50
Debt percentage steel (%)	38.45				
Debt percentage ammonia (%)		38.45			
Debt interest rate wind (%)	4.40	4.40	4.40	4.40	4.40
Debt interest rate PV (%)	4.40	4.40	4.40	4.40	4.40
Debt interest rate battery (%)	4.40	4.40	4.40	4.40	4.40
Debt interest rate electrolyzer (%)	4.40	4.40	4.40	4.40	4.40
Debt interest rate hydrogen storage (%)	4.40	4.40	4.40	4.40	4.40
Debt interest rate steel/ammonia (%)	5.00	5.00			
Months working reserve	1	1	1	1	1
Debt type	Revolving	Revolving	Revolving	Revolving	Revolving
Depr. method	MACRS	MACRS	MACRS	MACRS	MACRS
Depr. period (clean energy) (years)	5	5	5	5	5
Depr. period (hydrogen) (years)	7	7	7	7	7
Depr. period (steel/ammonia) (years)	7	7	7	7	7

Table 19. Normalized costs for individual subsystems. Values marked with an asterisk (*) were determined during the simulation as functions of other inputs.

ID	01	02	03	04	05
State	Minnesota	Texas	Texas	New Jersey	California
Area			Gulf Coast	New York Bight	
Product	Steel	Ammonia	Hydrogen	Hydrogen	Hydrogen
Wind CapEx (USD/kW)	1,380.00	1,380.00	2470.36*	2470.89*	4247.0*
Solar PV CapEx (USD/kW)	1,323.00	1,323.00	1,323.00	1,323.00	1,323.00
Battery CapEx (USD/kW)	311.00	311.00	311.00	311.00	311.00
Battery CapEx (USD/kWh)	310.00	310.00	310.00	310.00	310.00
PEM CapEx 1 MW system (USD/kW)	1295	1295	1295	1295	1295
Steel plant CapEx (USD/Mt)	592.5*				
Ammonia plant CapEx (USD/t)		289.99*			
Wind fixed O&M (USD/kW)	29	29	134.98*	145.05*	118.96*
Solar PV fixed O&M (USD/kW)	18	18	18	18	18
Battery fixed O&M (USD/kW)	15.53	15.53	38.77	38.77	38.77
Electrolyzer fixed O&M (USD/kW)	22.97*	22.97*	22.97*	22.97*	22.97*
Steel plant fixed O&M (USD/Mt)	103.41*				
Ammonia plant fixed O&M (USD/t)		32.67*			

3.3 Minnesota (Onshore/Steel)

Reference Design 01 is located in Minnesota. This system uses solar and wind energy to produce hydrogen through PEM electrolysis. The hydrogen then serves as a feedstock for steel production. See Table 17 for subsystem sizing. A high-level diagram of the reference design is shown in Figure 9, but this figure is intended primarily to show the relative size of the plant subsystems and should not be viewed as a final layout for construction.

The capital expense breakdown for the electricity/hydrogen and for the steel portions of the reference design are provided in Figures 10 and 11, respectively. Breakdowns of the levelized cost of hydrogen (LCOH) and levelized cost of steel (LCOS) are provided in Figures 12 and 13, respectively. Cash flows for the life of the plant are provided for the electricity/hydrogen and the steel portions of the reference design in Figures 14 and 15, respectively.

The energy generation and storage for a few hundred hours of operation are shown in Figure 16. The hydrogen production and storage for a year are shown in Figure 17. Different time frames were chosen for electricity and hydrogen because the hydrogen storage is a long-duration system, and the battery system is a short-duration storage system. Complete data are provided in the accompanying repository.

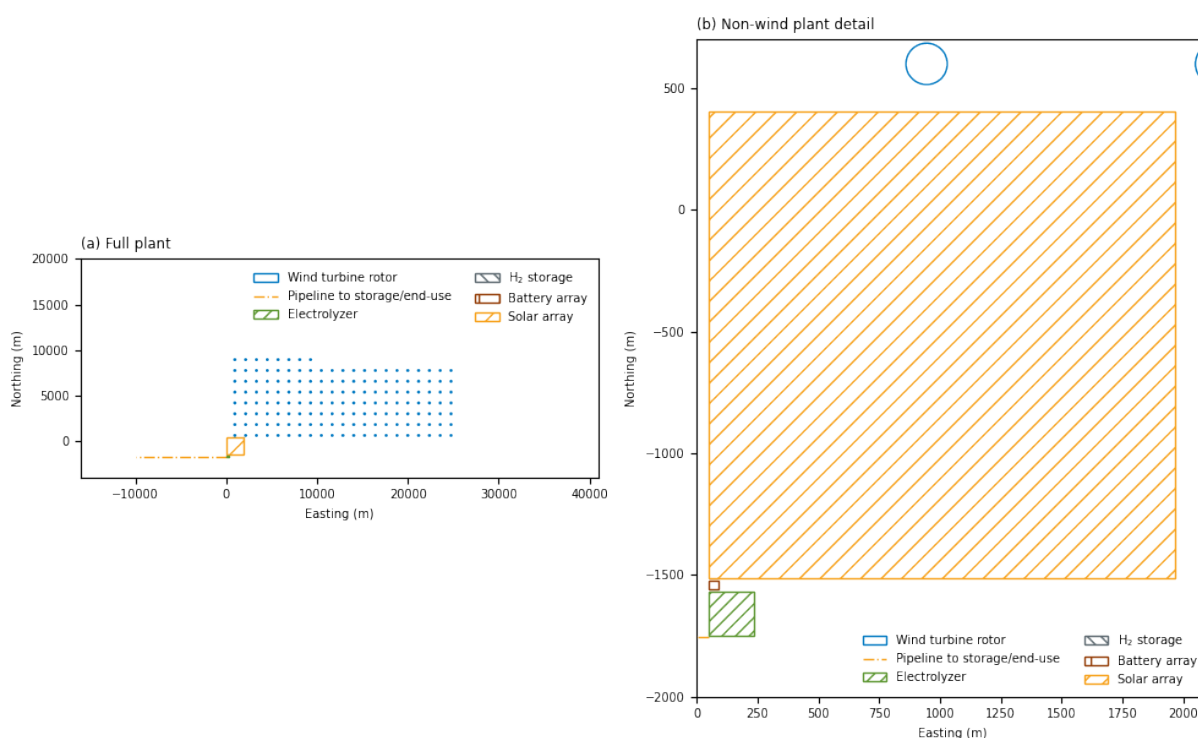


Figure 9. Rough depiction of system layout for Reference Design 01. This figure is intended to depict relative sizes of the plant components but not intended for use in actual construction.

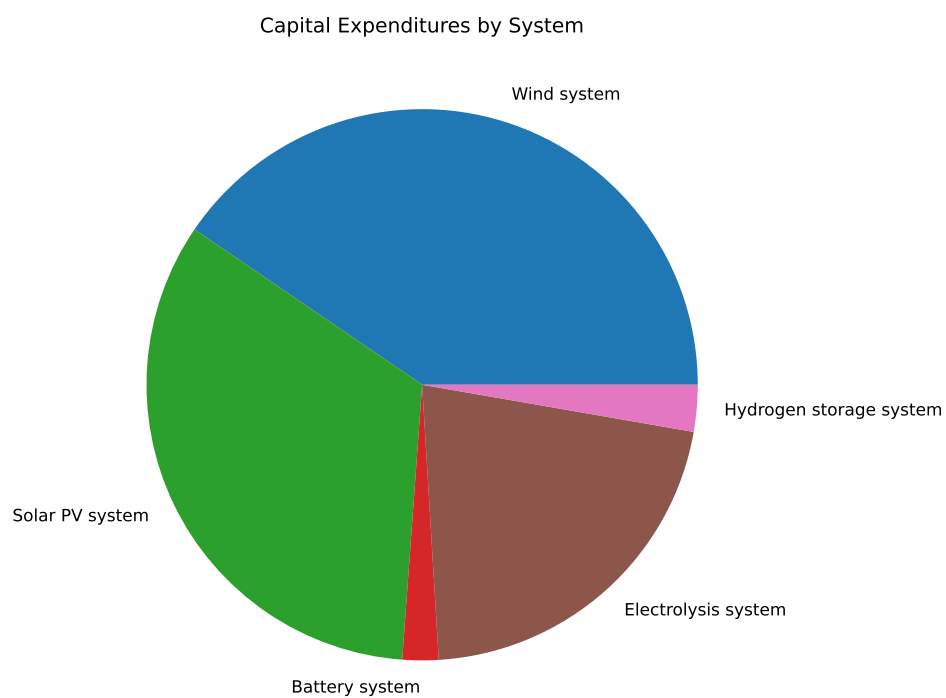


Figure 10. Capital expense breakdown for the electricity and hydrogen portions of Reference Design 01

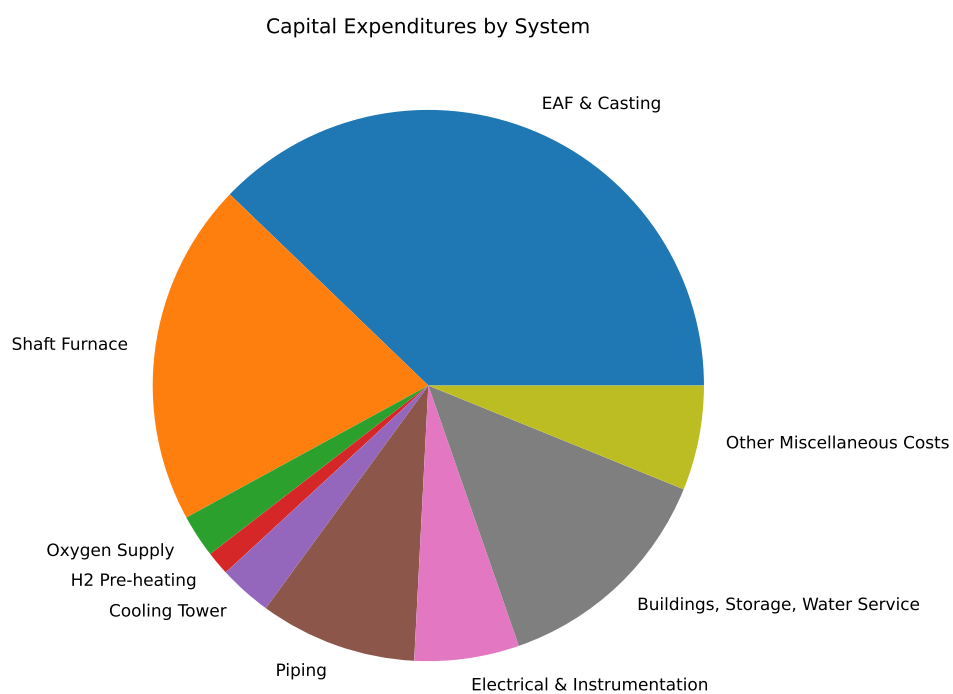


Figure 11. Capital expense breakdown for the steel plant portion of Reference Design 01

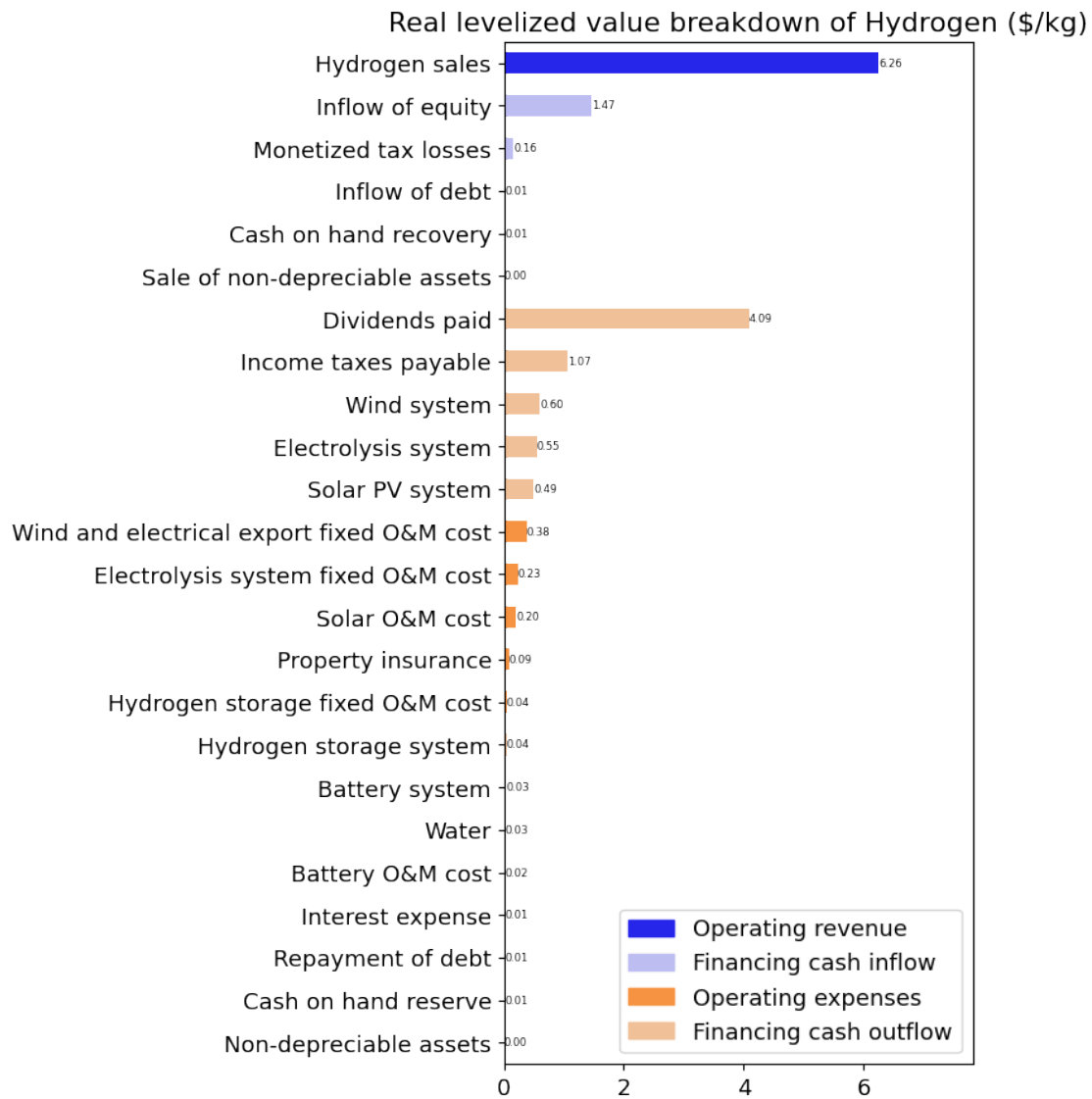


Figure 12. Levelized cost of hydrogen breakdown for Reference Design 01

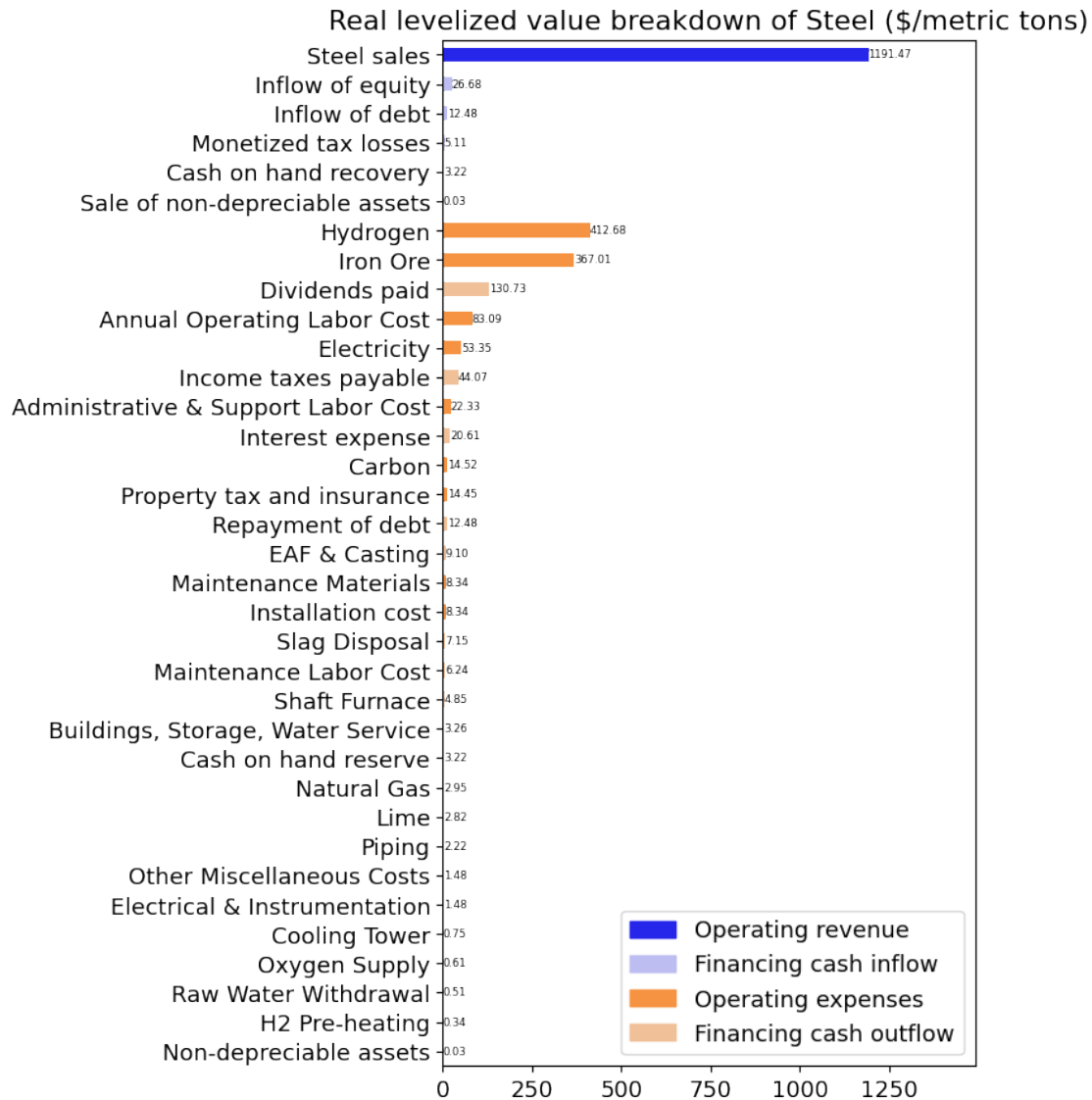


Figure 13. Levelized cost of steel breakdown for Reference Design 01

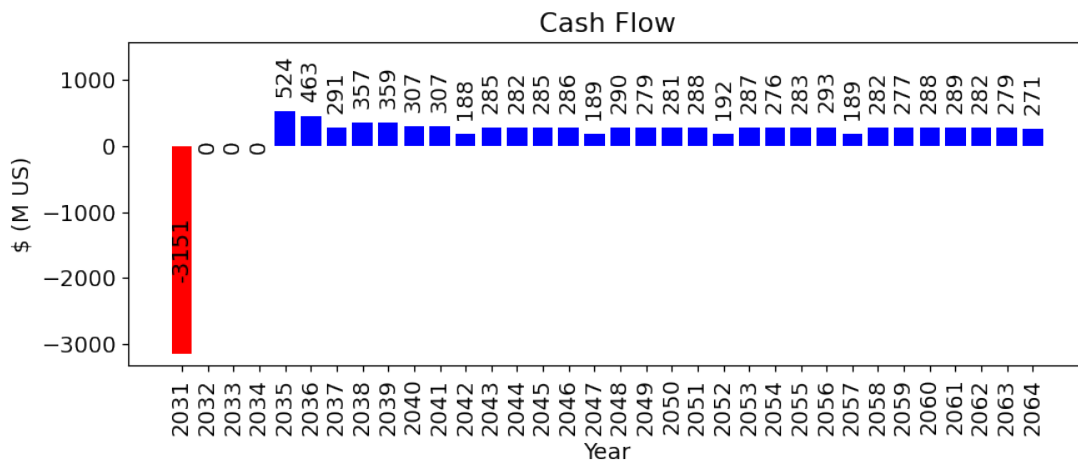


Figure 14. Cash flow for electricity and hydrogen portions of Reference Design 01

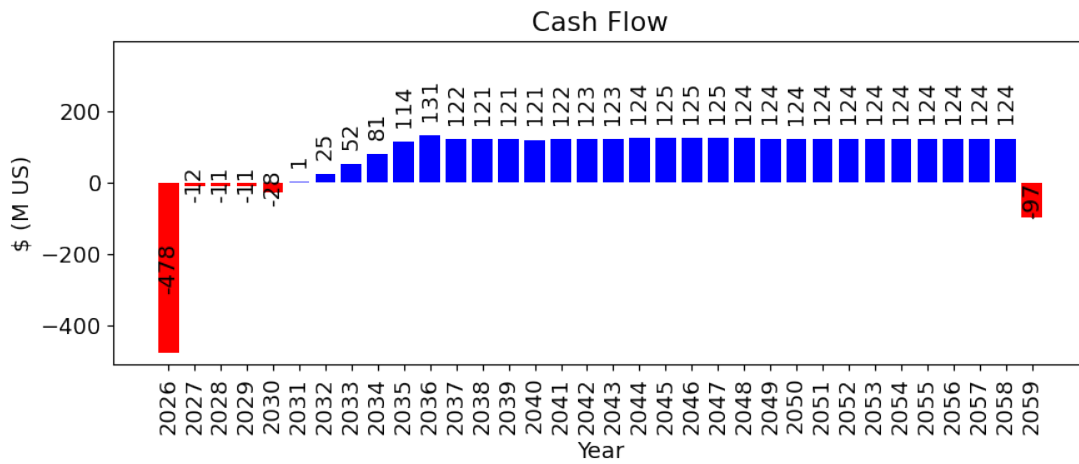


Figure 15. Cash flow for the steel plant portion of Reference Design 01

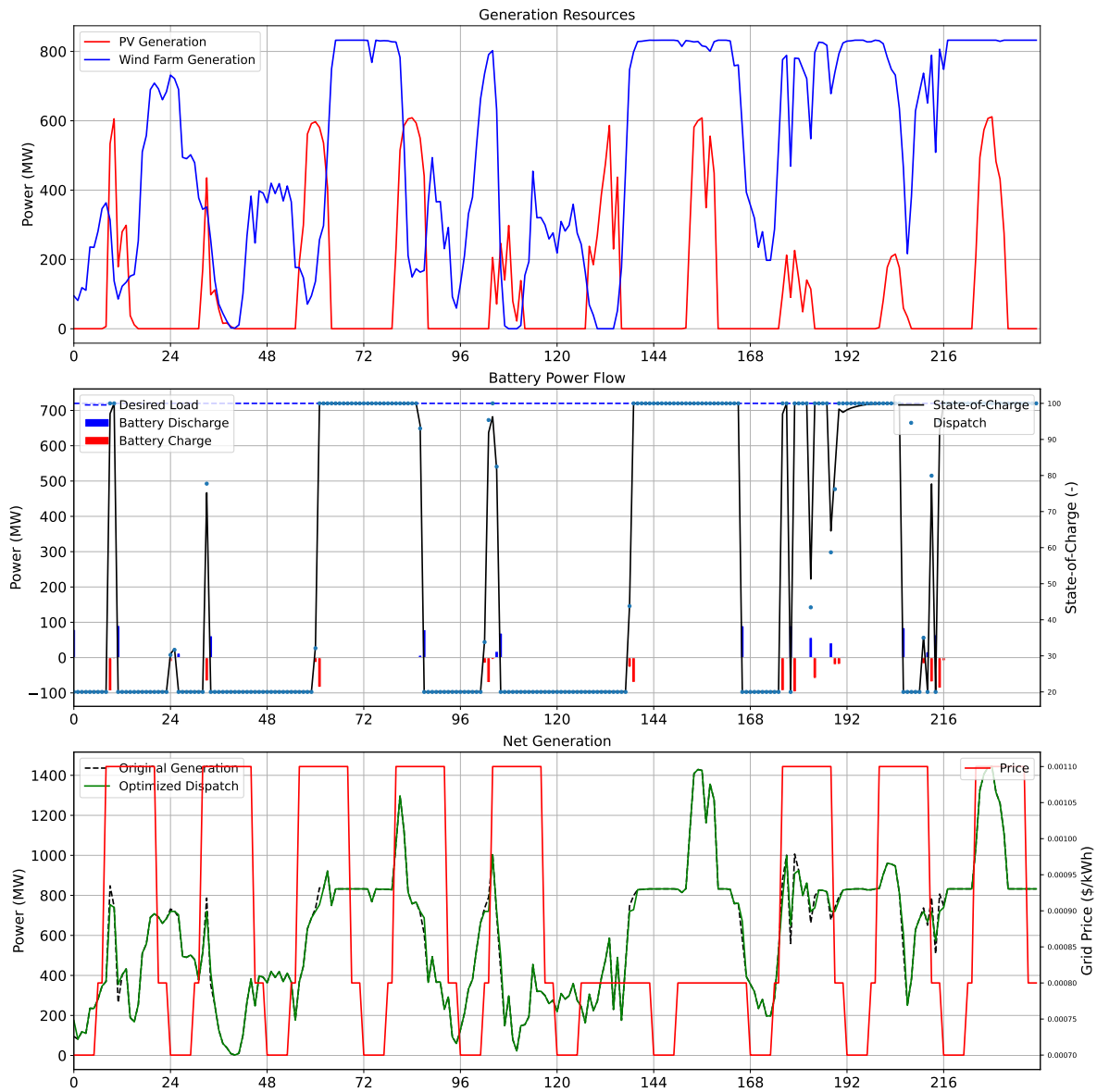


Figure 16. Renewable electricity generation and usage for Reference Design 01.
Complete data are provided in National Renewable Energy Laboratory (2025b).

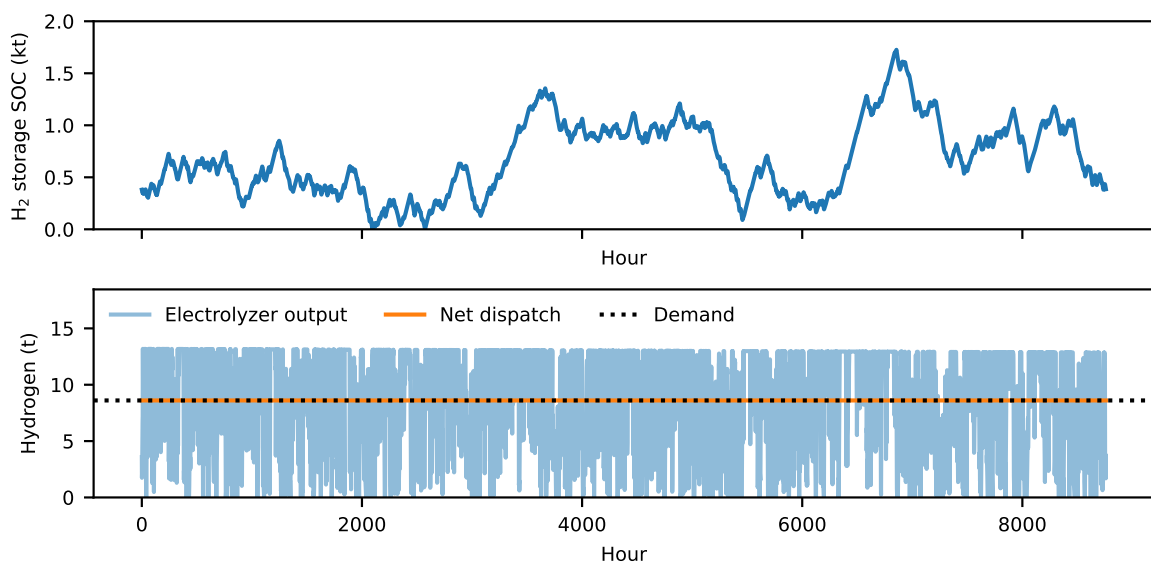


Figure 17. Hydrogen flow for Reference Design 01. Complete data are provided in National Renewable Energy Laboratory (2025b).

3.4 Texas (Onshore/Ammonia)

Reference Design 02 is located in Texas. This system uses solar and wind energy to produce hydrogen through PEM electrolysis. The hydrogen then serves as a feedstock for ammonia production. See Table 17 for subsystem sizing. A high-level diagram of the reference design is shown in Figure 18, but this figure is intended primarily to show the relative size of the plant subsystems and should not be viewed as a final layout for construction.

The capital expense breakdown for the electricity/hydrogen and for the steel portions of the reference design are provided in Figures 19 and 20, respectively. Breakdowns of the LCOH and levelized cost of ammonia (LCOA) are provided in Figures 21 and 22, respectively. Cash flows for the life of the plant are provided for the electricity/hydrogen and the steel portions of the reference design in Figures 23 and 24, respectively.

The energy generation and storage for a few hundred hours of operation are shown in Figure 25. The hydrogen production and storage for a year are shown in Figure 26. Different time frames were chosen for electricity and hydrogen because the hydrogen storage is a long-duration system, and the battery system is a short-duration storage system. Complete data are provided in the accompanying repository.

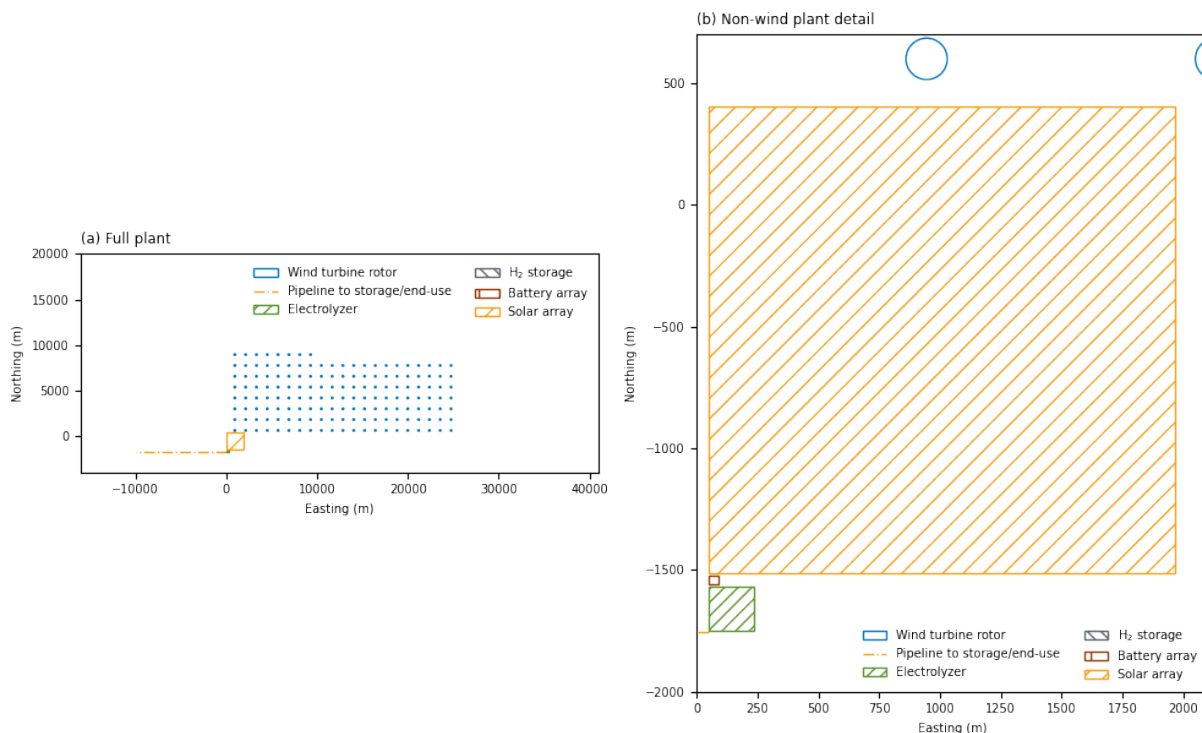


Figure 18. Rough depiction of system layout for Reference Design 02. This figure is intended to depict relative sizes of the plant components but not intended for use in actual construction.

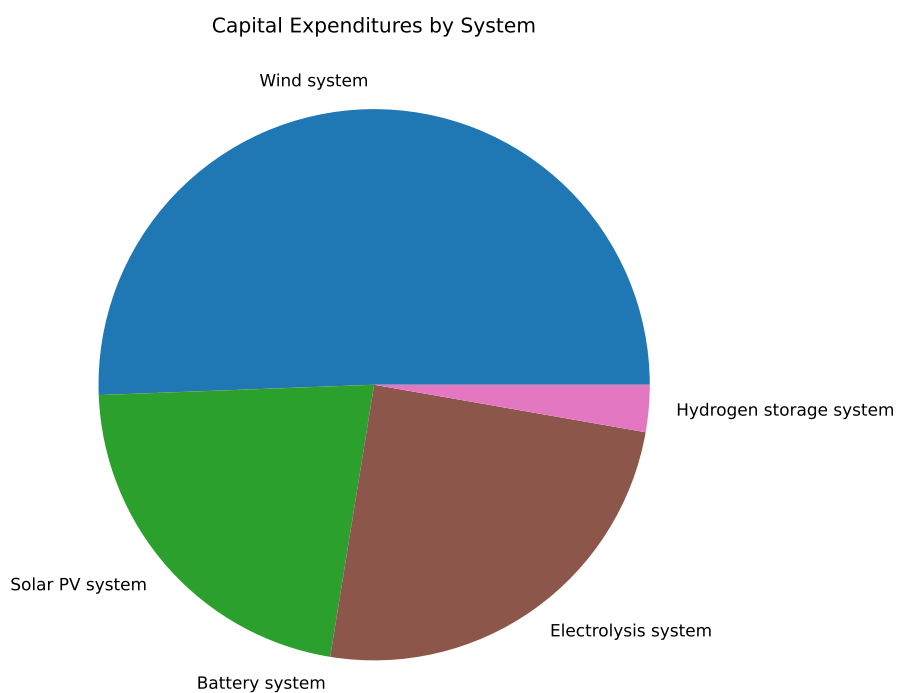


Figure 19. Capital expense breakdown for the electricity and hydrogen portions of Reference Design 02

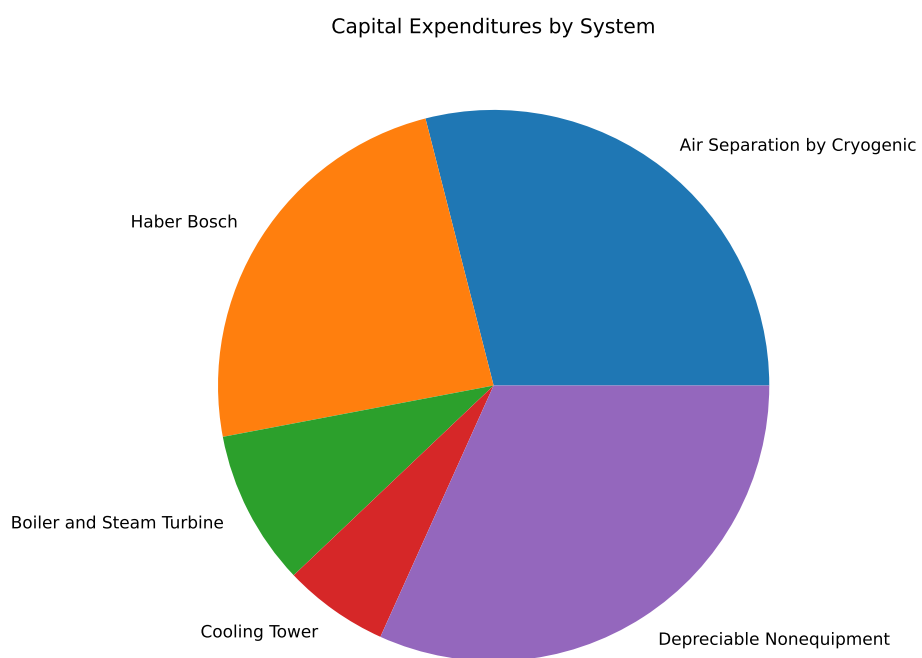


Figure 20. Capital expense breakdown for the ammonia plant portion of Reference Design 02

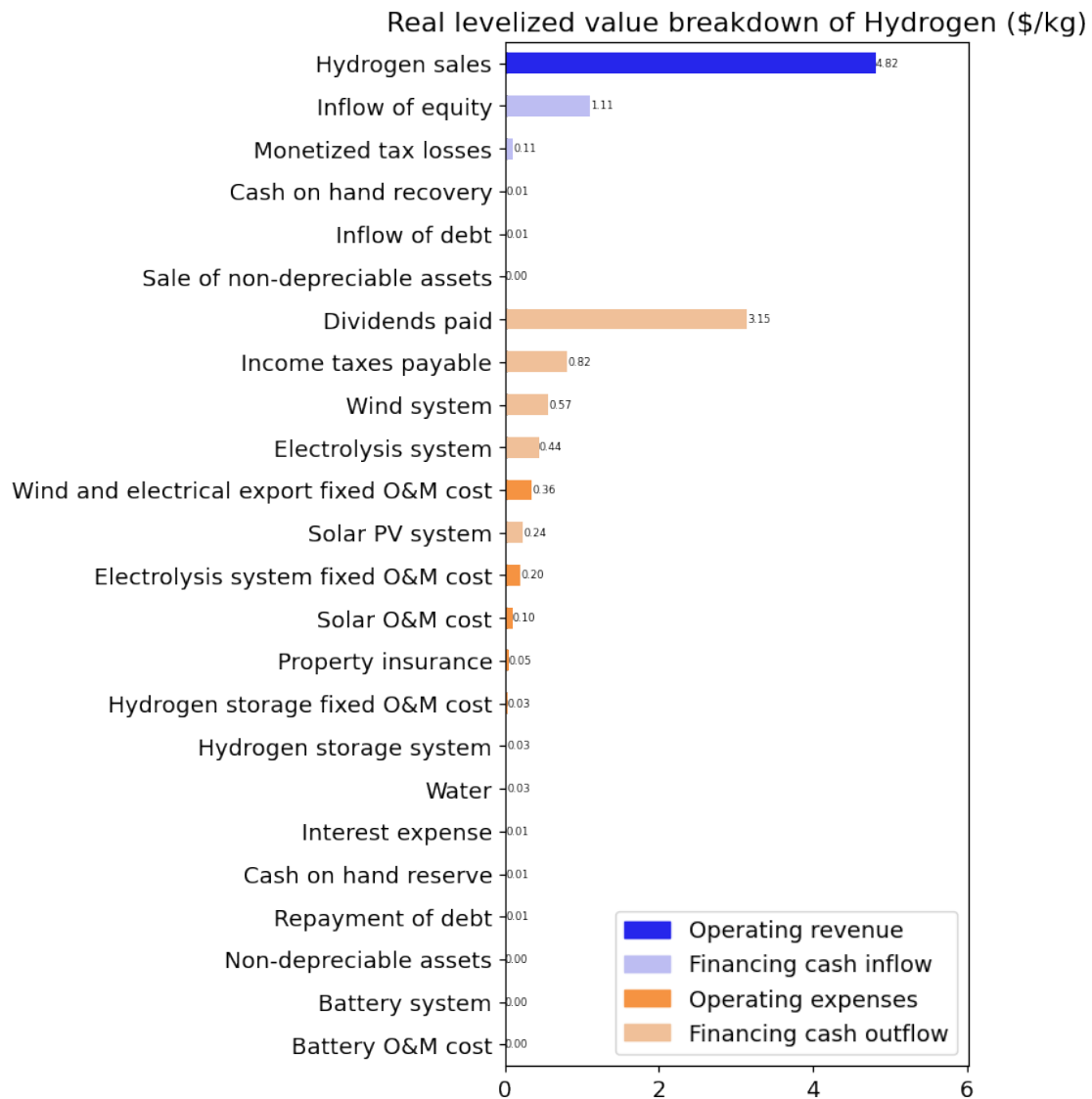


Figure 21. Levelized cost of hydrogen breakdown for Reference Design 02



Figure 22. Levelized cost of ammonia breakdown for Reference Design 02

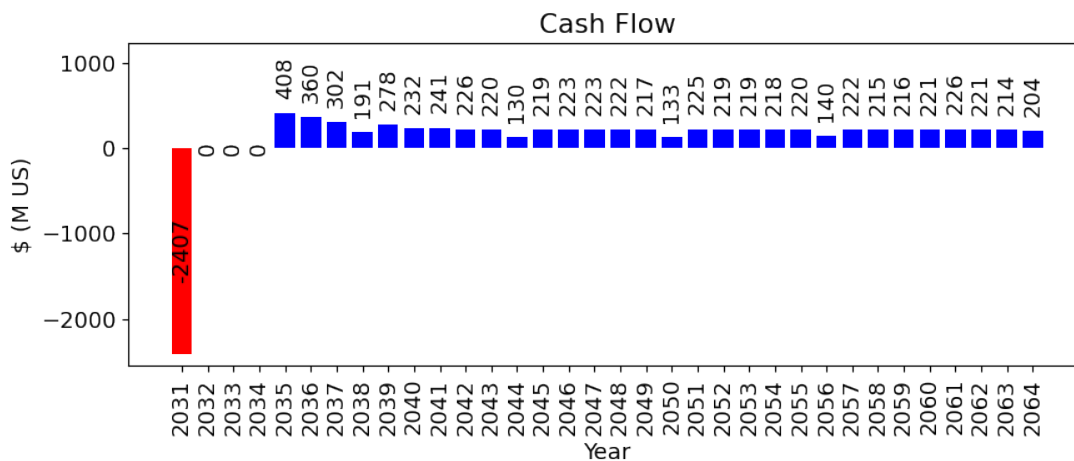


Figure 23. Cash flow for electricity and hydrogen portions of Reference Design 02

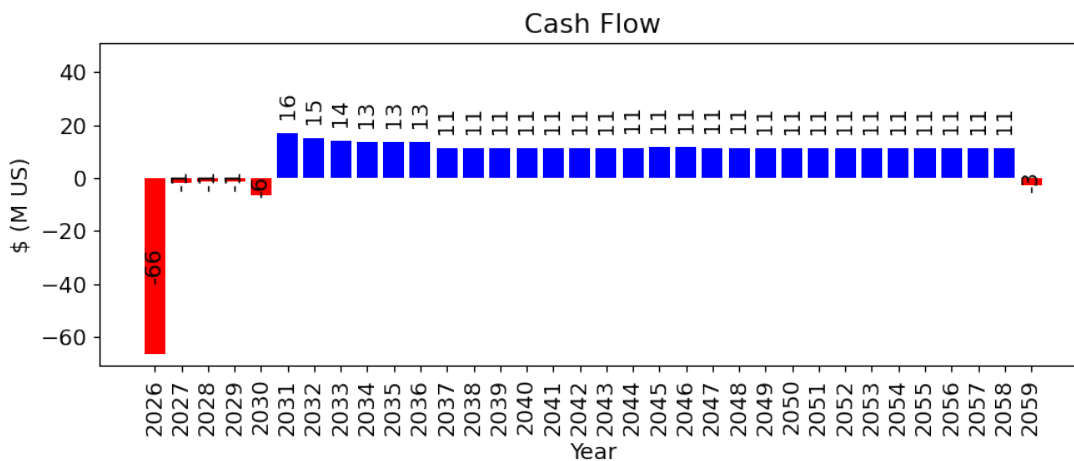


Figure 24. Cash flow for the ammonia plant portion of Reference Design 02

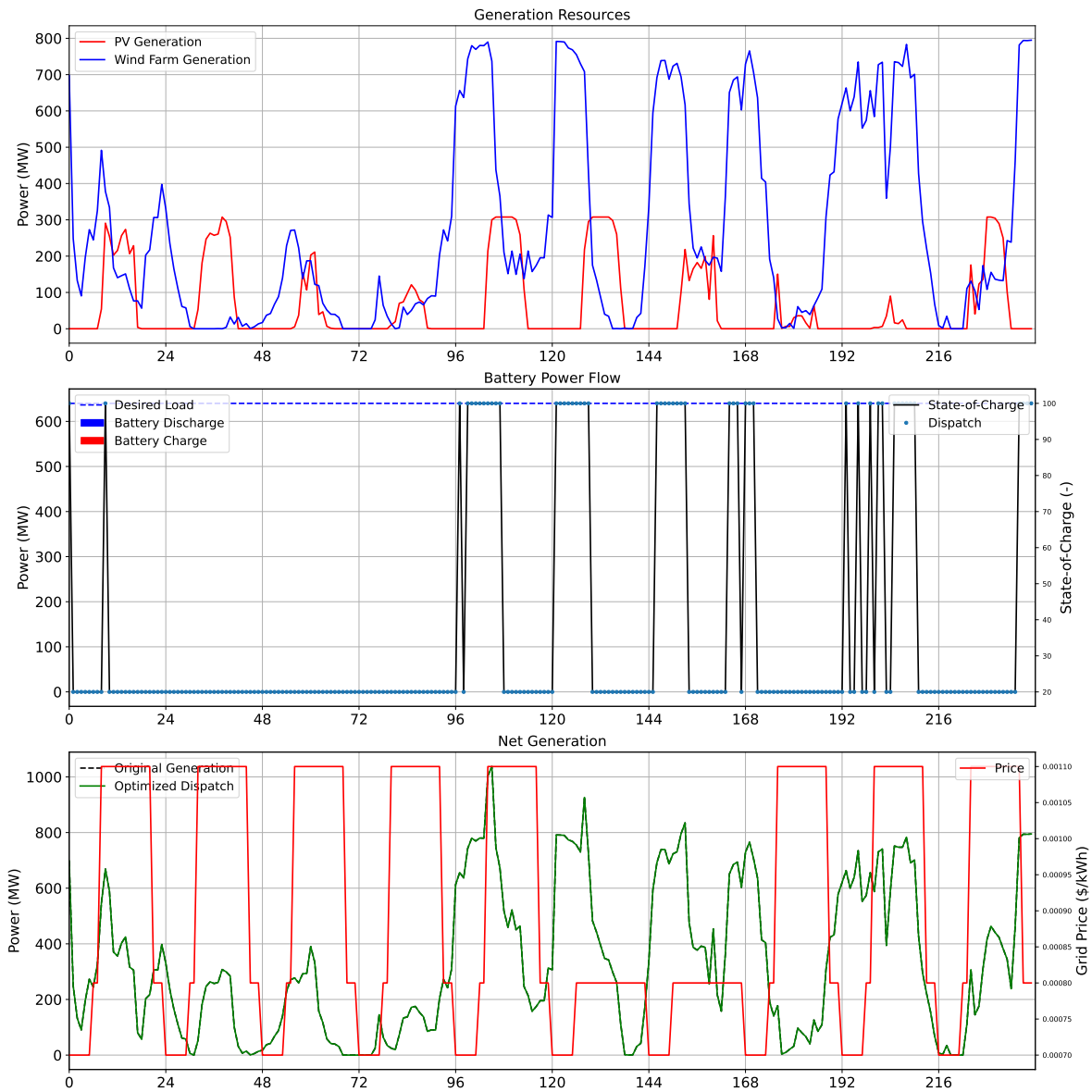


Figure 25. Renewable electricity generation and usage for Reference Design 02.
Complete data are provided in National Renewable Energy Laboratory (2025b).

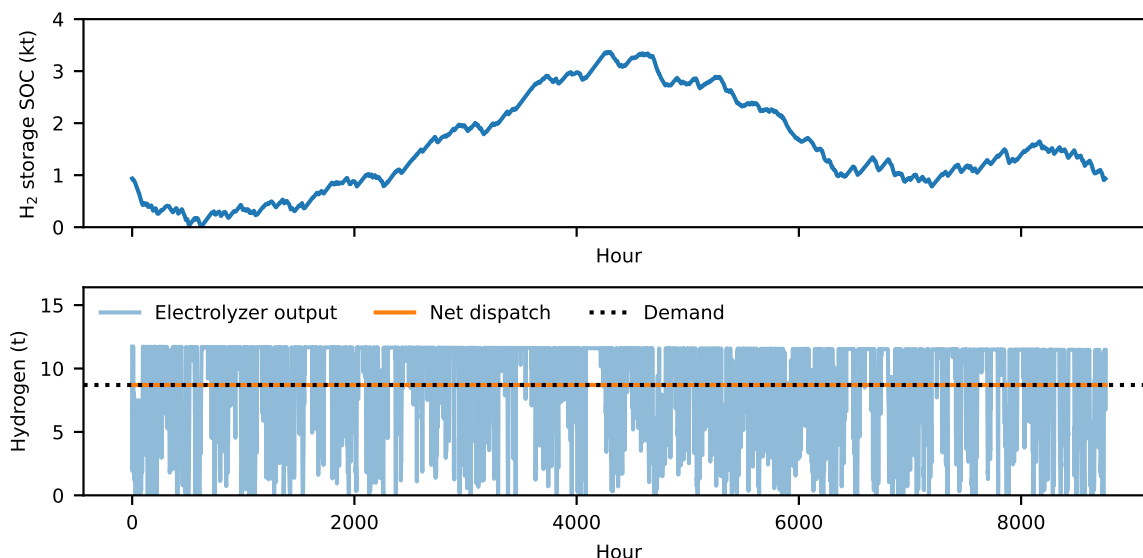


Figure 26. Hydrogen flow for Reference Design 02. Complete data are provided in National Renewable Energy Laboratory (2025b).

3.5 Texas, Gulf Coast (Fixed Offshore Wind With Onshore Hydrogen)

Reference Design 03 is located in Texas on and near the Gulf Coast. This system uses solar and wind energy to produce hydrogen through PEM electrolysis. The wind farm is located offshore using fixed foundations while the rest of the hybrid system is located onshore (see Figure 5). This reference design uses cables A1 and A2 for the wind farm array cables and cable E1 for the export cables (see Table 3). A high-level diagram of the reference design is shown in Figure 27, but this figure is intended primarily to show the relative size of the plant subsystems and should not be viewed as a final layout for construction.

The capital expense breakdown for the system is provided in Figure 28. A breakdown of the LCOH is provided in Figure 29. Cash flows for the life of the plant are provided for the reference design in Figure 30.

The energy generation and storage for a few hundred hours of operation are shown in Figure 31. The hydrogen production and storage for a year are shown in Figure 32. Different time frames were chosen for electricity and hydrogen because the hydrogen storage is a long-duration system, and the battery system is a short-duration storage system. Complete data are provided in the accompanying repository.

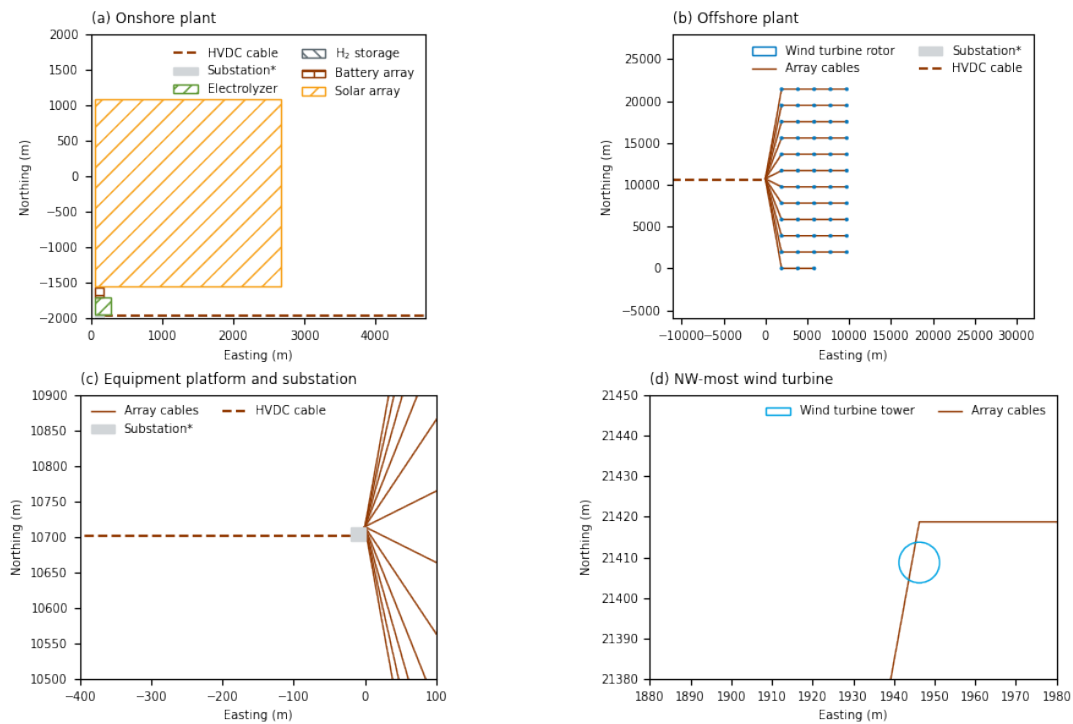


Figure 27. Rough depiction of system layout for Reference Design 03. This figure is intended to depict relative sizes of the plant components but not intended for use in actual construction.

Capital Expenditures by System

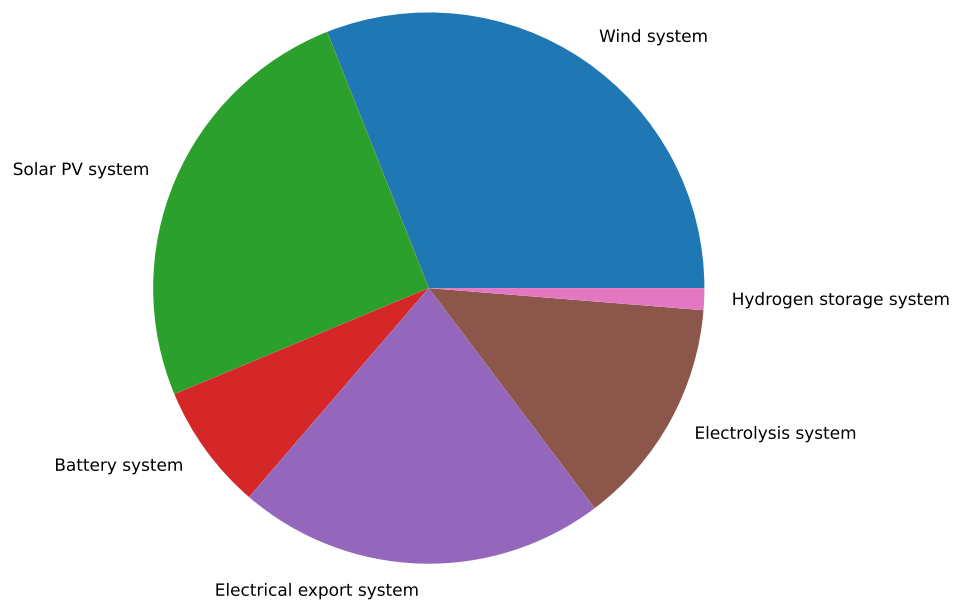


Figure 28. Capital expense breakdown for Reference Design 03

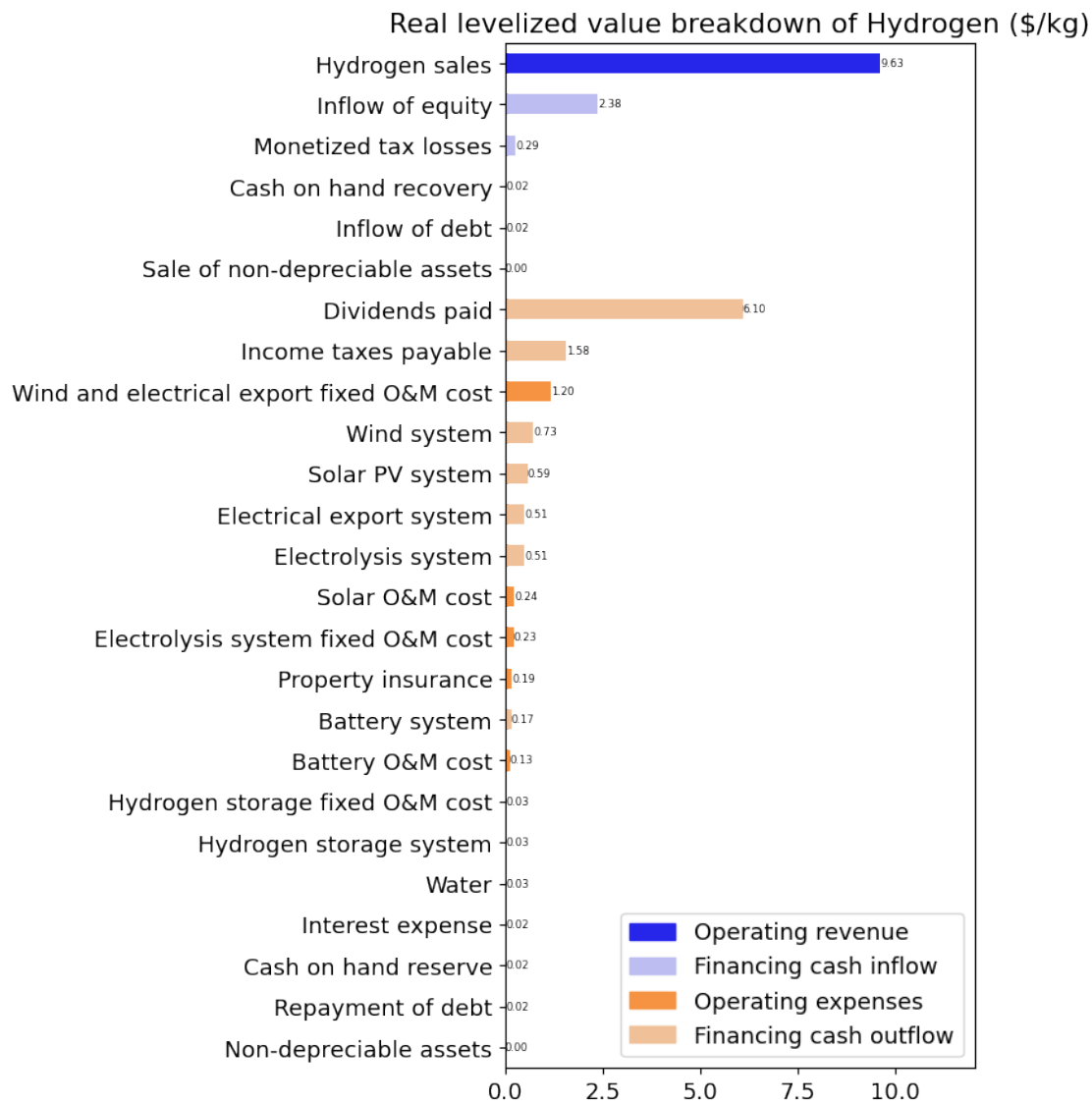


Figure 29. Levelized cost of hydrogen breakdown for Reference Design 03

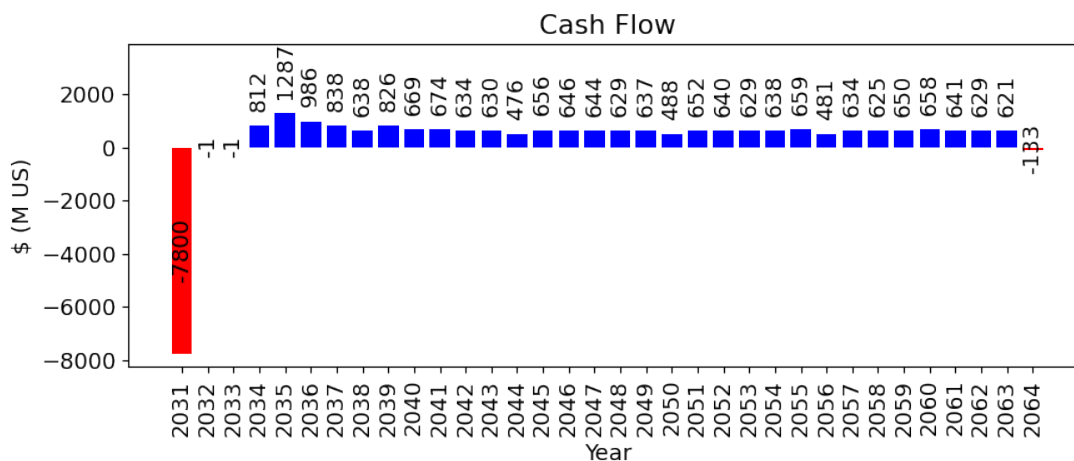


Figure 30. Cash flow for Reference Design 03

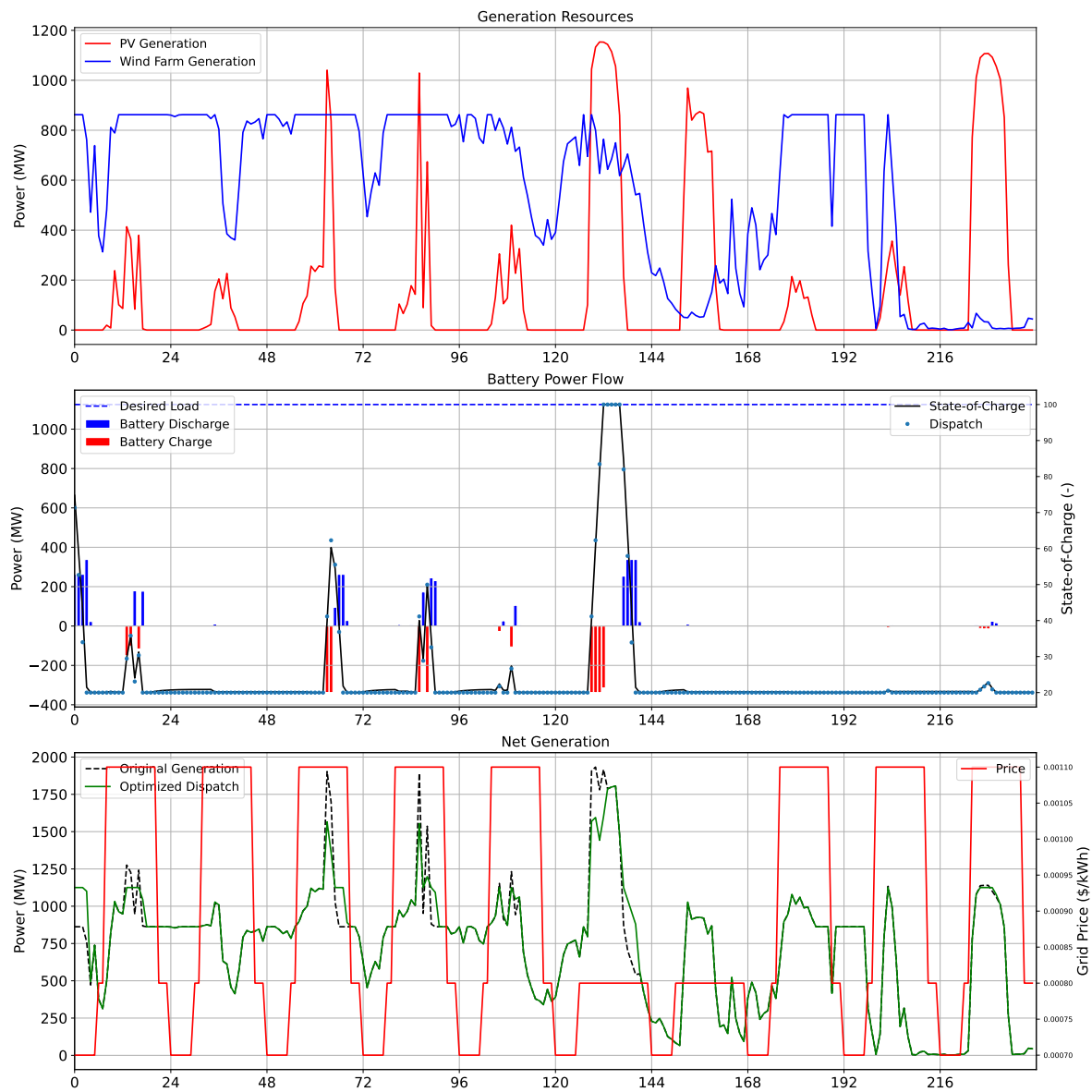


Figure 31. Renewable electricity generation and usage for Reference Design 03.
Complete data are provided in National Renewable Energy Laboratory (2025b).

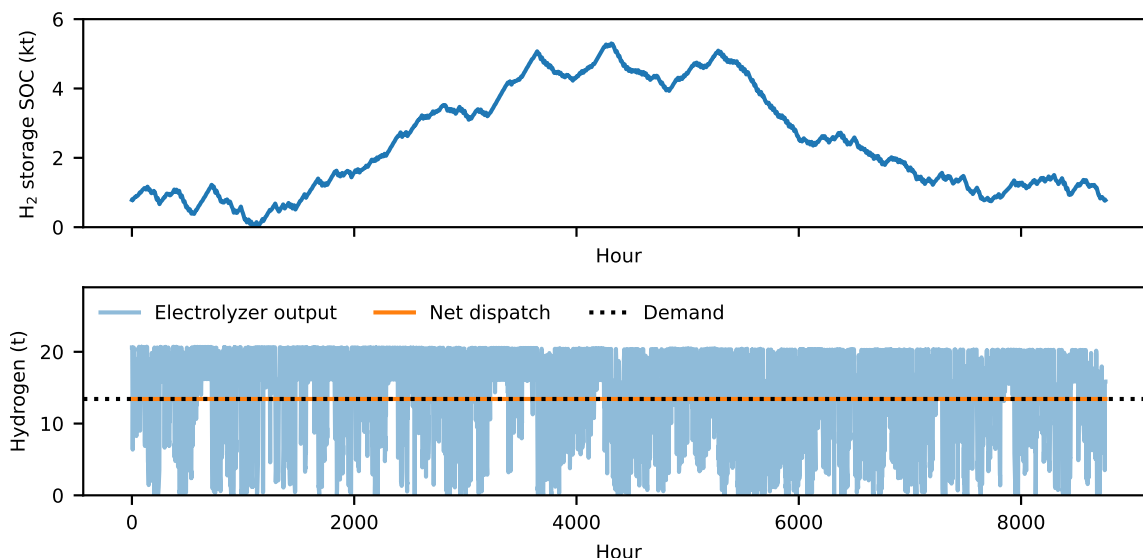


Figure 32. Hydrogen flow for Reference Design 03. Complete data are provided in National Renewable Energy Laboratory (2025b).

3.6 New York Bight (Fixed Offshore Wind With Onshore Hydrogen)

Reference Design 04 is located in New Jersey (onshore subsystems) and the New York Bight (offshore wind). This system uses solar and wind energy to produce hydrogen through PEM electrolysis. The wind farm is located offshore using fixed foundations while the rest of the hybrid system is located onshore (see Figure 5). This reference design uses cables A1 and A2 for the wind farm array cables and cable E2 for the export cables (see Table 3). A high-level diagram of the reference design is shown in Figure 33, but this figure is intended primarily to show the relative size of the plant subsystems and should not be viewed as a final layout for construction.

The capital expense breakdown for the system is provided in Figure 34. A breakdown of the LCOH is provided in Figure 35. Cash flows for the life of the plant are provided for the reference design in Figure 36.

The energy generation and storage for a few hundred hours of operation are shown in Figure 37. The hydrogen production and storage for a year are shown in Figure 38. Different time frames were chosen for electricity and hydrogen because the hydrogen storage is a long-duration system, and the battery system is a short-duration storage system. Complete data are provided in the accompanying repository.

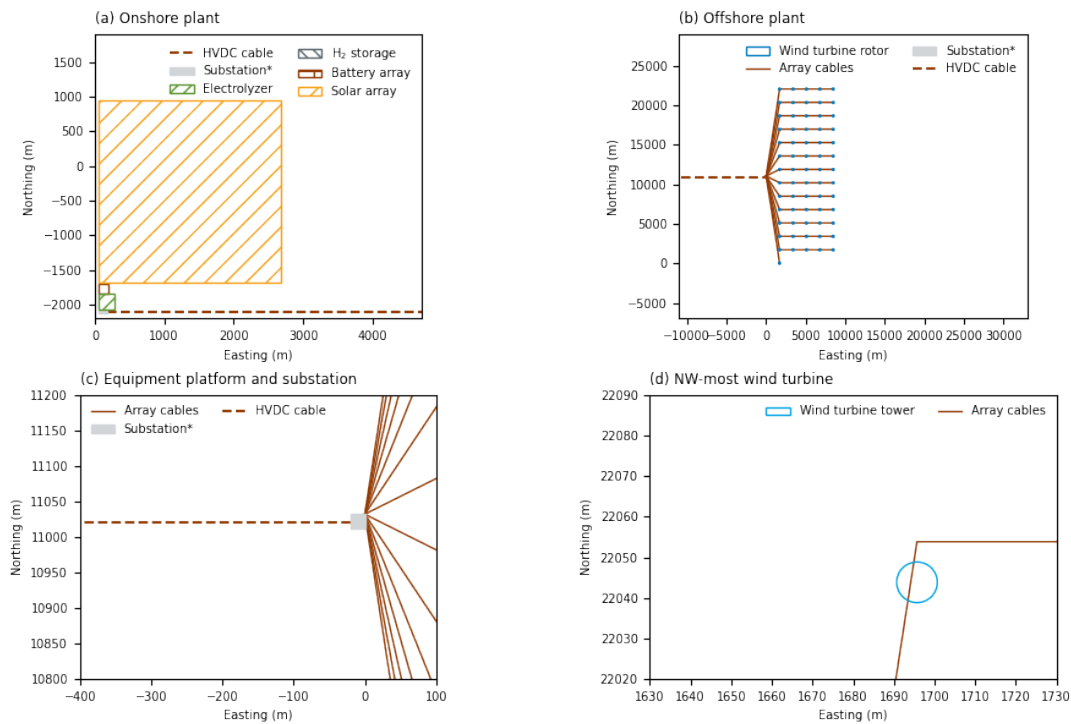


Figure 33. Rough depiction of system layout for Reference Design 04. This figure is intended to depict relative sizes of the plant components but not intended for use in actual construction.

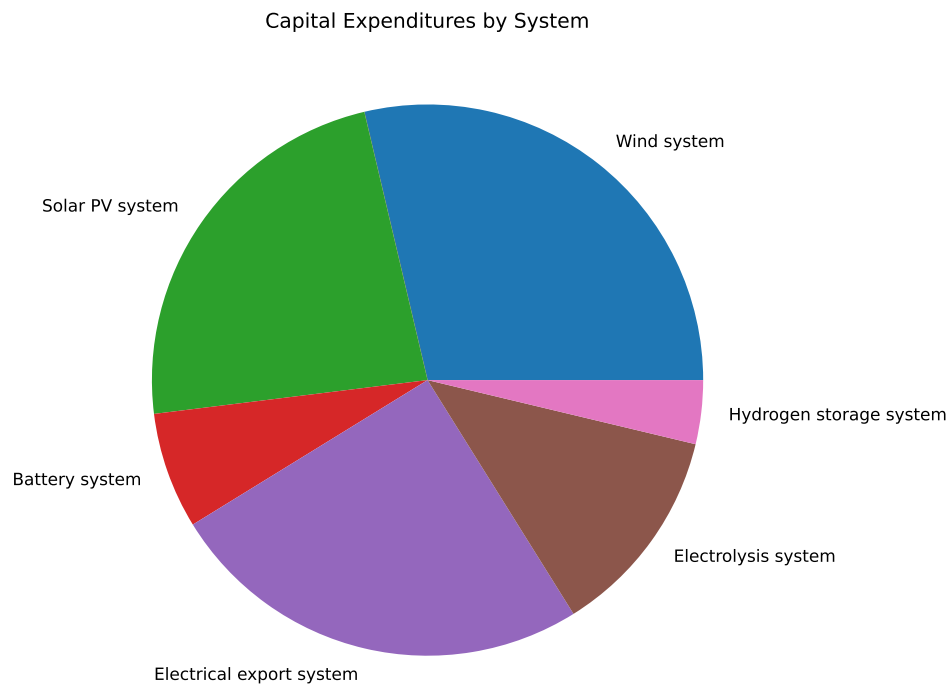


Figure 34. Capital expense breakdown for Reference Design 04

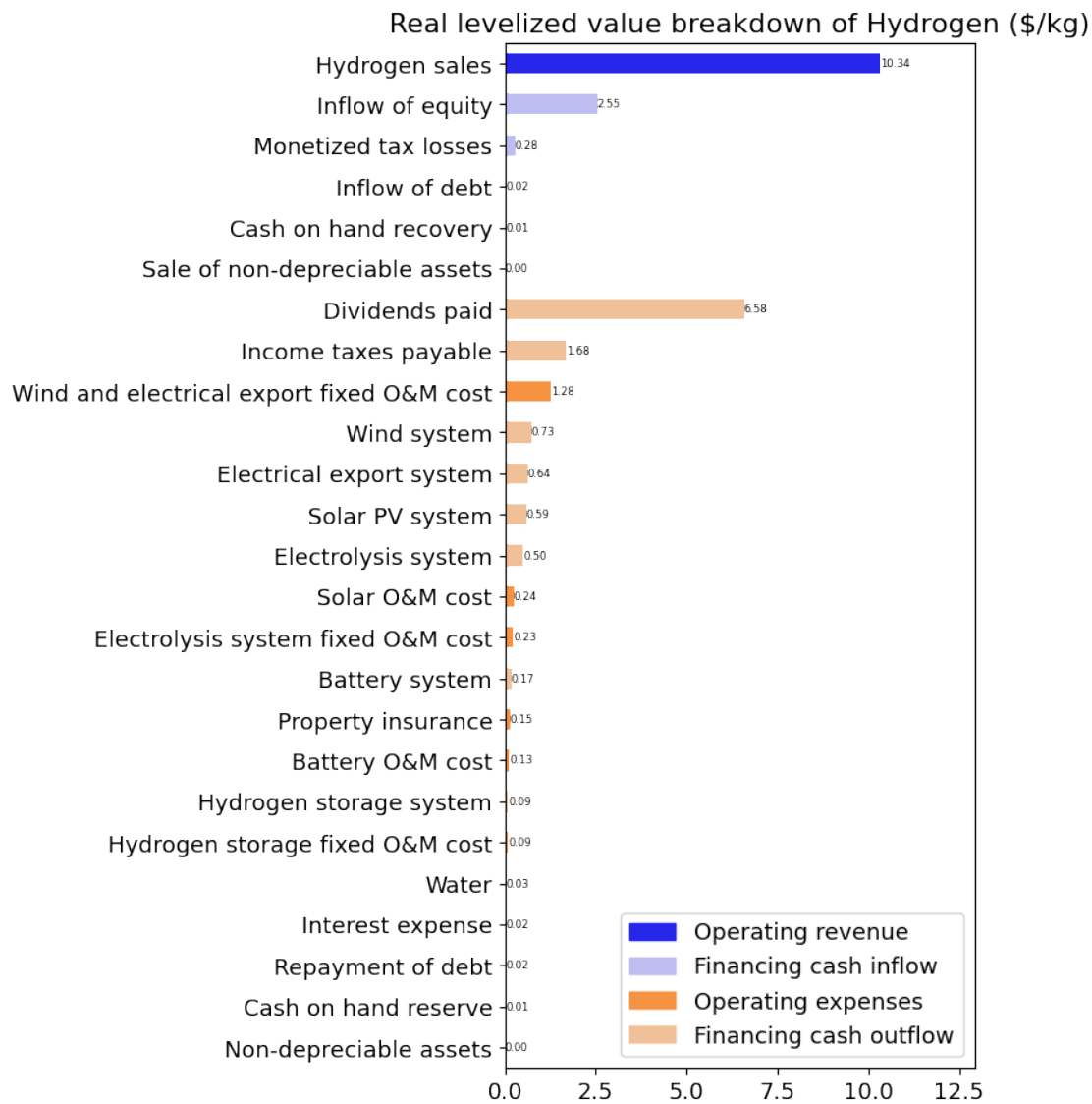


Figure 35. Levelized cost of hydrogen breakdown for Reference Design 04

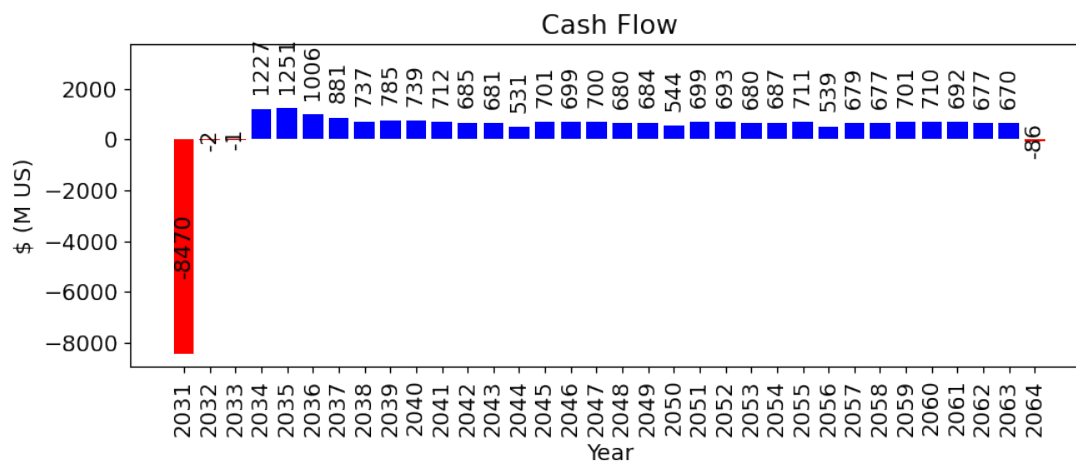


Figure 36. Cash flow for Reference Design 04

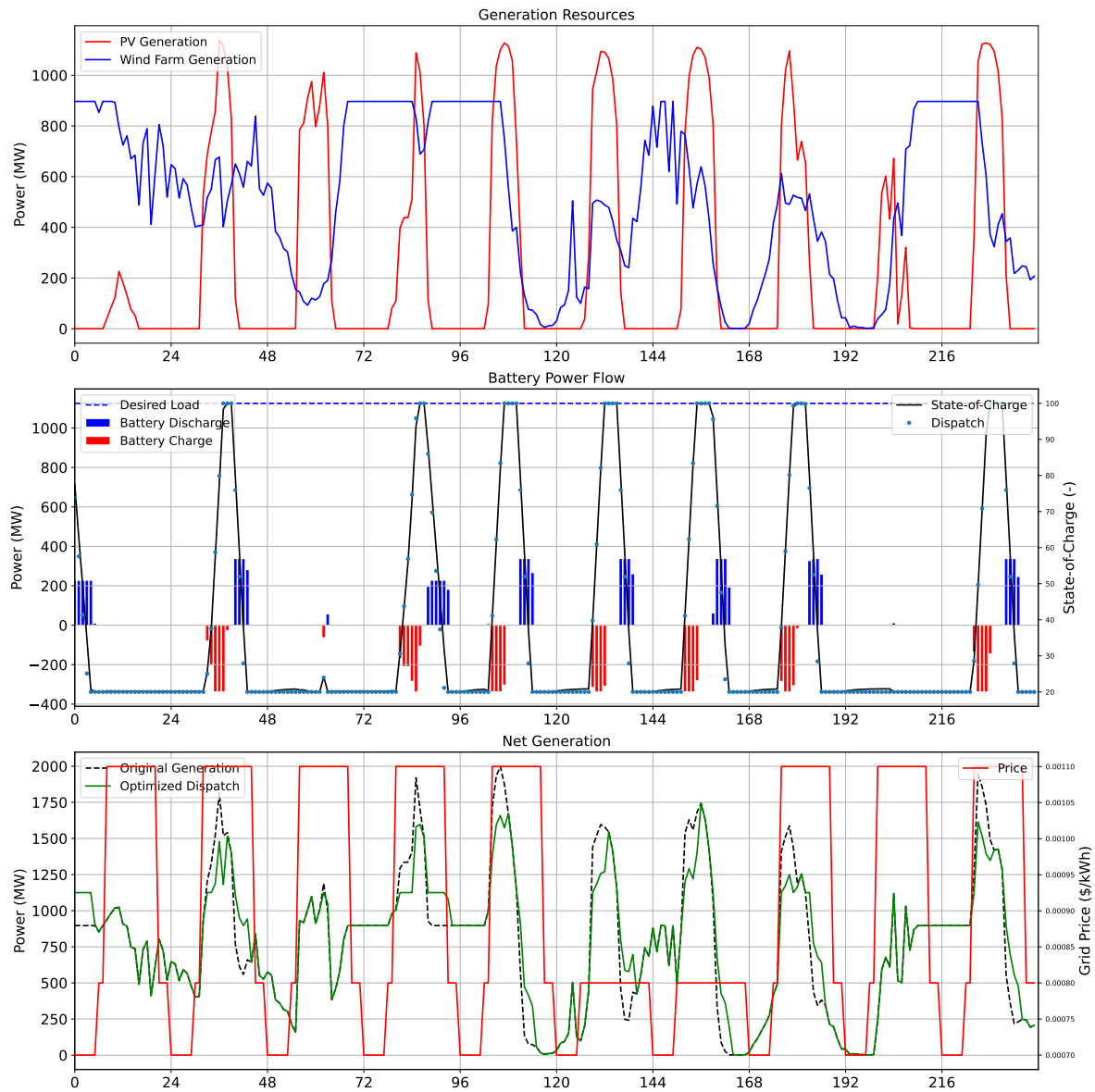


Figure 37. Renewable electricity generation and usage for Reference Design 04.
Complete data are provided in National Renewable Energy Laboratory (2025b).

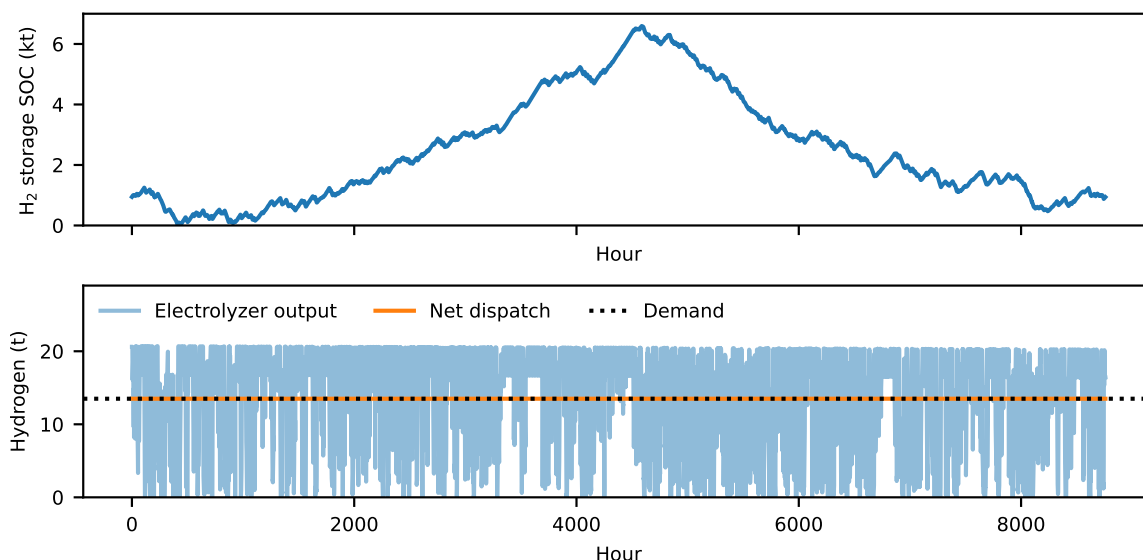


Figure 38. Hydrogen flow for Reference Design 04. Complete data are provided in (National Renewable Energy Laboratory 2025b).

3.7 California (Floating Offshore Wind With Onshore Hydrogen)

Reference Design 05 is located in California on and near the coast. This system uses solar and wind energy to produce hydrogen through PEM electrolysis. The wind farm is located offshore using floating foundations while the rest of the hybrid system is located onshore (see Figure 5). This reference design uses cables A3 and A4 for the wind farm array cables and cable E3 for the export cables (see Table 3). A high-level diagram of the reference design is shown in Figure 39, but this figure is intended primarily to show the relative size of the plant subsystems and should not be viewed as a final layout for construction.

The capital expense breakdown for the system is provided in Figure 40. A breakdown of the LCOH is provided in Figure 41. Cash flows for the life of the plant are provided for the reference design in Figure 42.

The energy generation and storage for a few hundred hours of operation are shown in fig. 43. The hydrogen production and storage for a year are shown in fig. 44. Different time frames were chosen for electricity and hydrogen because the hydrogen storage is a long-duration system, and the battery system is a short-duration storage system. Complete data are provided in the accompanying repository.

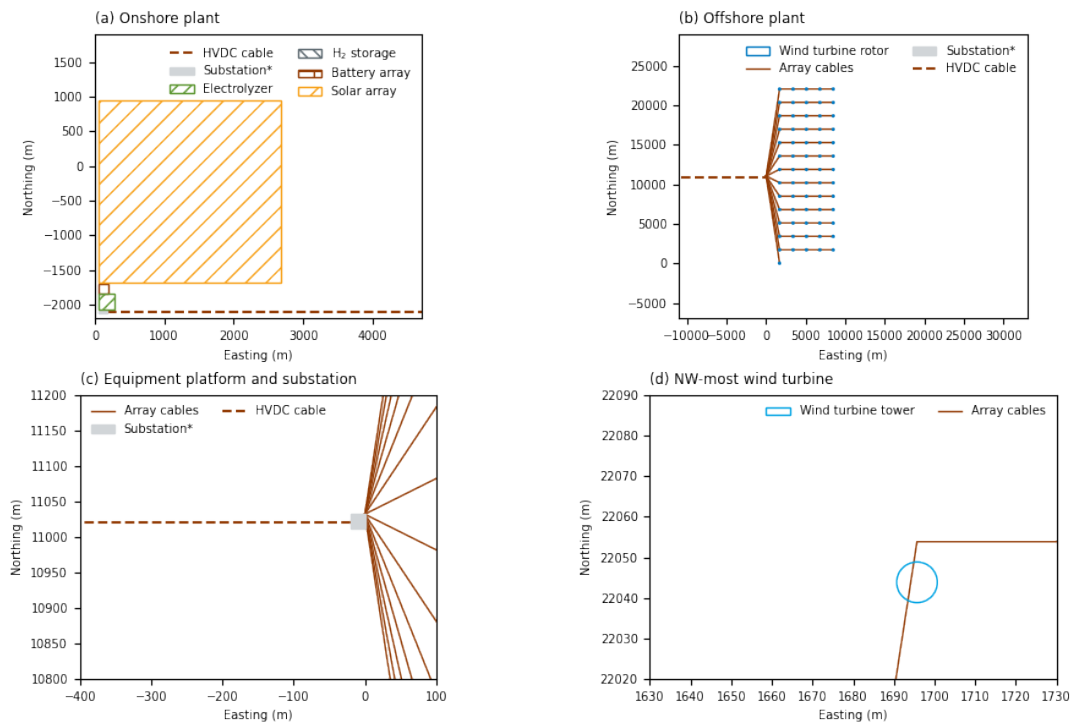


Figure 39. Rough depiction of system layout for Reference Design 05. This figure is intended to depict relative sizes of the plant components but not intended for use in actual construction.

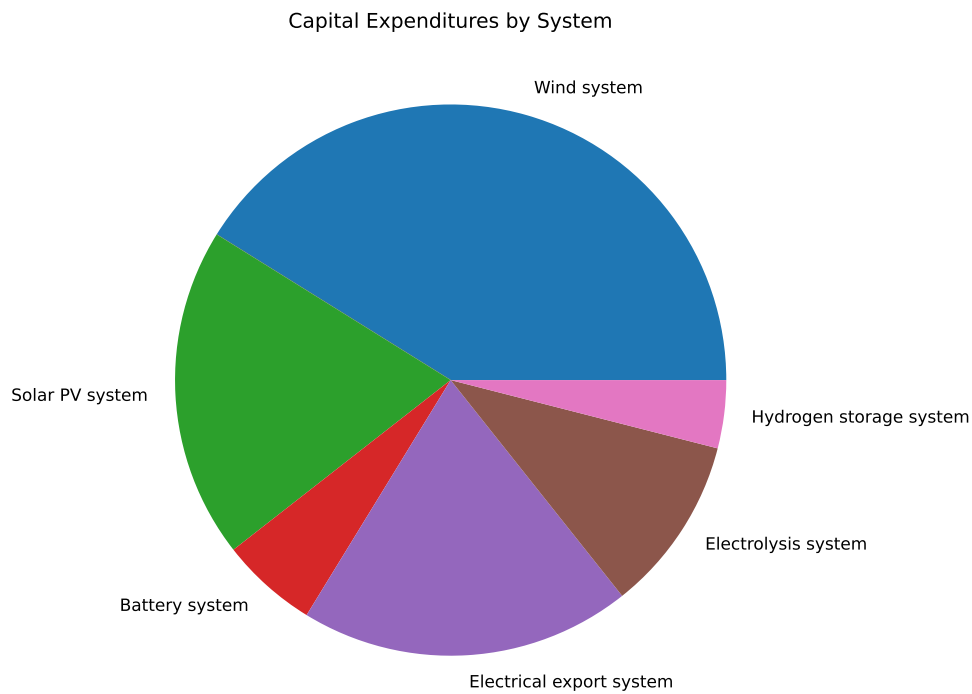


Figure 40. Capital expense breakdown for Reference Design 05

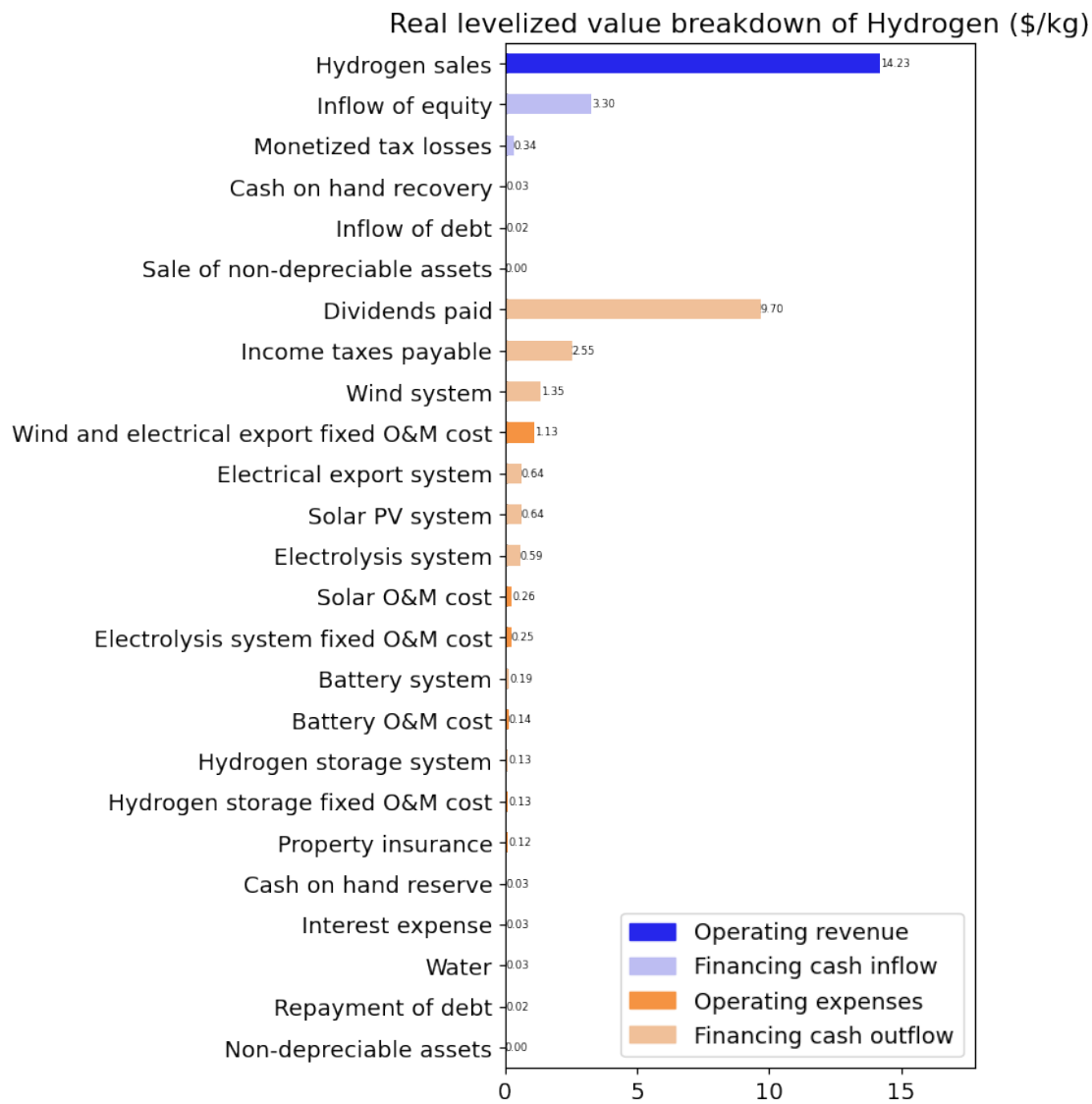


Figure 41. Levelized cost of hydrogen breakdown for Reference Design 05

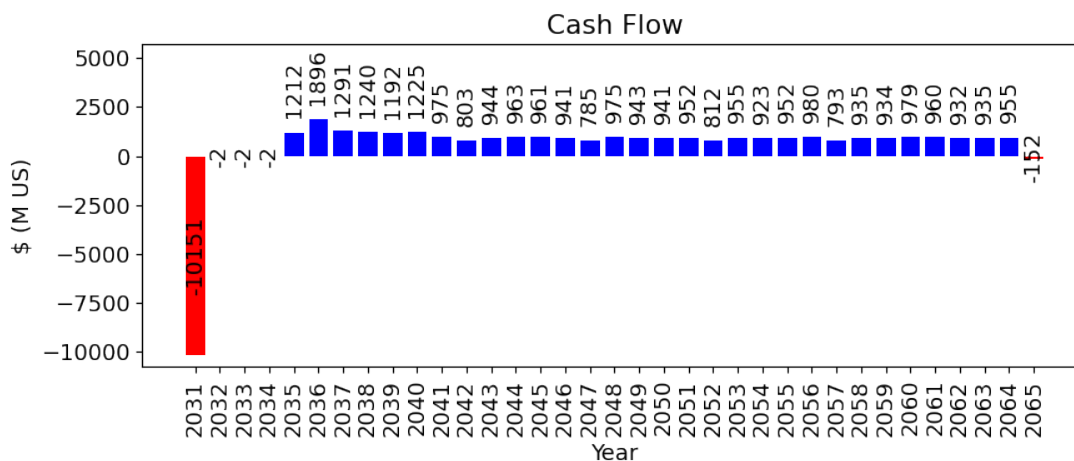


Figure 42. Cash flow for Reference Design 05

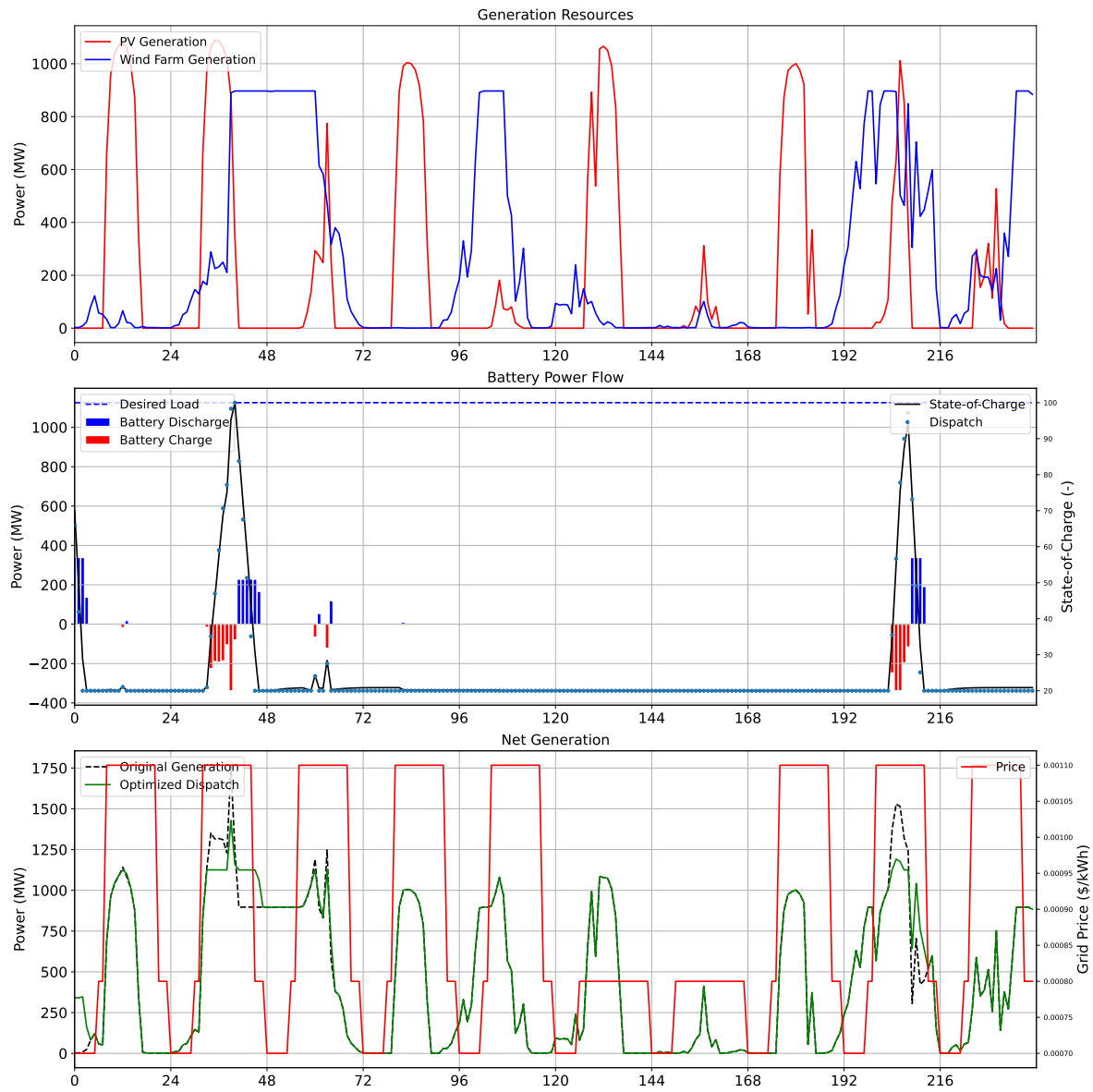


Figure 43. Renewable electricity generation and usage for Reference Design 05.
Complete data are provided in National Renewable Energy Laboratory (2025b).

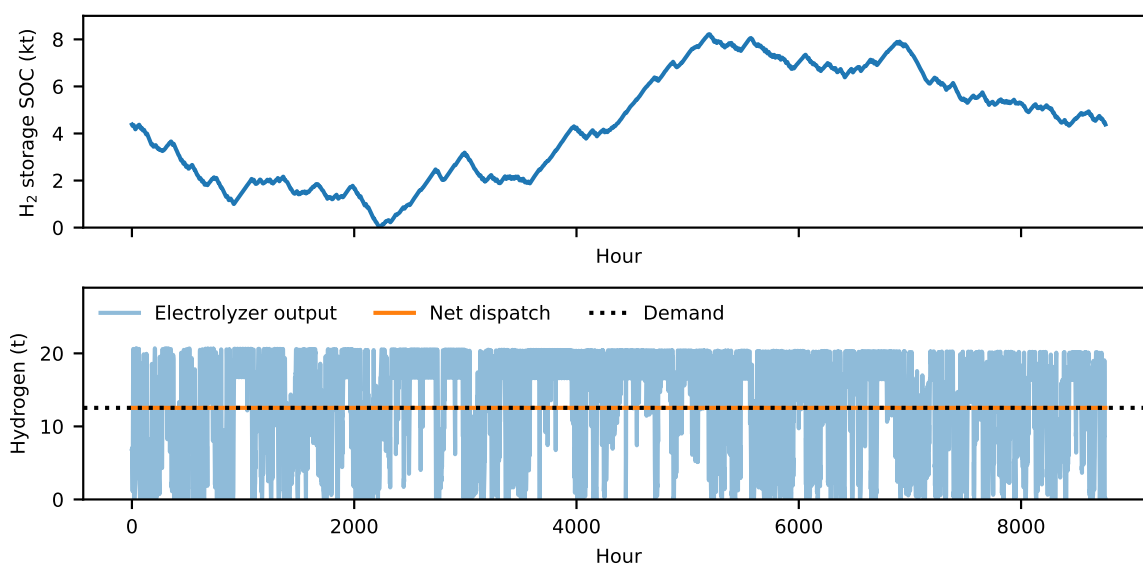


Figure 44. Hydrogen flow for Reference Design 05. Complete data are provided in National Renewable Energy Laboratory (2025b).

References

- American Iron and Steel Institute. 2023. *AISI Releases Annual Statistical Report for 2022*. <https://www.steel.org/2023/06/aisi-releases-annual-statistical-report-for-2022/>.
- Argonne National Laboratory. 2023. *Hydrogen Delivery Scenario Analysis Model*. 4.0. Accessed November 30, 2023. <https://hdsam.es.anl.gov/index.php?content=hdsam>.
- Danecek, P., J. Bonfield, J. Liddle, J. Marshall, V. Ohan, M. Pollard, A. Whitwham, et al. 2021. “Twelve years of SAMtools and BCFtools.” *Gigascience*, <https://doi.org/10.1093/gigascience/giab008>.
- Decarbonization Technology. 2023. *Hydrogen derivatives key to the global renewable energy trade*. <https://decarbonizationtechnology.com/article/188/hydrogen-derivatives-key-to-the-global-renewable-energy-trade>.
- Eberle, A., T. Mai, O. Roberts, T. Williams, P. Pinchuk, A. Lopez, M. Mowers, J. Mowers, T. Stehly, and E. Lantz. 2024. *Incorporating Wind Turbine Choice in High-Resolution Geospatial Supply Curve and Capacity Expansion Models*. Technical report. National Renewable Energy Laboratory (NREL), Golden, CO (United States).
- EIA. 2023. *Annual Energy Outlook 2023*. <https://www.eia.gov/outlooks/aeo/data/browser/>. Online; accessed November 2023.
- Fuchs, R., W. Musial, G. R. Zuckerman, M. Chetan, M. Marquis, L. Rese, A. Cooperman, P. Duffy, R. Green, P. Beiter, et al. 2023. *Assessment of Offshore Wind Energy Opportunities and Challenges in the US Gulf of Mexico*. Technical report. National Renewable Energy Laboratory (NREL), Golden, CO (United States).
- Fuchs, R., G. R. Zuckerman, P. Duffy, M. Shields, W. Musial, P. Beiter, A. Cooperman, and S. Bredenkamp. 2024. “The Cost of Offshore Wind Energy in the United States From 2025 to 2050” (August). <https://doi.org/10.2172/2433785>. <https://www.osti.gov/biblio/2433785>.
- Gaertner, E., J. Rinker, L. Sethuraman, F. Zahle, B. Anderson, G. E. Barter, N. J. Abbas, F. Meng, P. Bortolotti, W. Skrzypinski, et al. 2020. *IEA wind TCP task 37: definition of the IEA 15-megawatt offshore reference wind turbine*. Technical report. National Renewable Energy Lab.(NREL), Golden, CO (United States).
- Geeraad, P., P. Fleming, S. A. Ning, and J.-W. van Wingerden. 2014. *FLORIS*, May. <https://www.osti.gov/biblio/1262644>.
- Hall, M., S. Housner, S. Srinivas, and S. Wilson. 2021. *MoorPy (Quasi-Static Mooring Analysis in Python)*. [Computer Software] <https://doi.org/10.11578/dc.20210726.1>, July. <https://doi.org/10.11578/dc.20210726.1>.
- Hamilton, W., J. Martinek, J. Cox, and A. Newman. 2022. “Integrating Concentrating Solar Power Technologies into the Hybrid Optimization and Performance Platform (HOPP)” (August). <https://doi.org/10.2172/1884793>. <https://www.osti.gov/biblio/1884793>.
- Hamilton, W. T., M. A. Husted, A. M. Newman, R. J. Braun, and M. J. Wagner. 2020. “Dispatch optimization of concentrating solar power with utility-scale photovoltaics.” *Optimization and Engineering* 21, no. 1 (March): 335–369. ISSN: 1573-2924. <https://doi.org/10.1007/s11081-019-09449-y>. <https://doi.org/10.1007/s11081-019-09449-y>.
- Harrison-Atlas, D., C. Murphy, A. Schleifer, and N. Grue. 2022. “Temporal complementarity and value of wind-PV hybrid systems across the United States.” *Renewable Energy* 201:111–123. ISSN: 0960-1481. <https://doi.org/https://doi.org/10.1016/j.renene.2022.10.060>. <https://www.sciencedirect.com/science/article/pii/S0960148122015531>.
- Hydrogen Delivery Scenario Analysis Model*. V. 3.1. Accessed November 30, 2023. <https://hdsam.es.anl.gov/index.php?content=hdsam>.
- International Renewable Energy Agency. 2022. *Renewable Power Generation. Costs in 2021*. https://www.irena.org/-/media/Files/IRENA/Agency/Publication/2022/Jul/IRENA_Power_Generation_Costs_2021.pdf?rev=34c22a4b244d434da0accde7de7c73d8. Online; accessed January 2023.

Jonkman, J. 2009. “Definition of a 5-MW Reference Wind Turbine for Offshore System Development.” *National Renewable Energy Laboratory*.

Kee, J., and M. (Penev. 2023. *ProFAST (Production Financial Analysis Scenario Tool) [SWR-23-88]*. [Computer Software] <https://doi.org/10.11578/dc.20231211.1>, November. <https://doi.org/10.11578/dc.20231211.1>.

Lambe, A. B., and J. R. R. A. Martins. 2012. “Extensions to the Design Structure Matrix for the Description of Multidisciplinary Design, Analysis, and Optimization Processes.” *Structural and Multidisciplinary Optimization* 46:273–284. <https://doi.org/10.1007/s00158-012-0763-y>.

Lee, K., X. Liu, P. Vyawahare, P. Sun, A. Elgowainy, and M. Wang. 2022. “Techno-economic performances and life cycle greenhouse gas emissions of various ammonia production pathways including conventional, carbon-capturing, nuclear-powered, and renewable production.” *Green Chem.* 24 (12): 4830–4844. <https://doi.org/https://doi.org/10.1039/d2gc00843b>.

Maness, M., B. Maples, and A. Smith. 2017. *NREL offshore balance-of-system model*. Technical report. National Renewable Energy Lab.(NREL), Golden, CO (United States).

National Renewable Energy Laboratory. 2023. *PySAM Version 4.2.0*. Golden, CO. github.com/nrel/pysam.

———. 2024. *Annual Technology Baseline*. <https://atb.nrel.gov/>. Golden, CO.

———. 2025a. *GreenHEART*. V0.1.x. Golden, CO. <https://github.com/NREL/GreenHEART>.

———. 2025b. *Reference Hybrid System Designs*. <https://github.com/NREL/ReferenceHybridSystemDesigns>.

Nunemaker, J., M. Shields, R. Hammond, and P. Duffy. 2020. *ORBIT: Offshore Renewables Balance-of-system and Installation Tool*. Technical report NREL/TP-5000-77081. <https://www.nrel.gov/docs/fy20osti/77081.pdf>; National Renewable Energy Laboratory.

Papadimas, D., and R. Ahluwalia. 2021. “Bulk storage of hydrogen.” *International Journal of Hydrogen Energy* 46 (70): 34527–34541. ISSN: 0360-3199. <https://doi.org/https://doi.org/10.1016/j.ijhydene.2021.08.028>.

Reznicek, E. P., M. N. Koleva, J. King, M. Kotarbinski, E. Grant, S. Vijayshankar, K. Brunik, et al. 2024. “Techno-economic analysis of low-carbon hydrogen production pathways for decarbonizing steel and ammonia production.” Accepted, *Cell Reports Sustainability*.

Rosner, F., D. Papadimas, K. Brooks, K. Yoro, R. K. Ahluwalia, T. Autrey, and H. Breunig. 2023a. “Green steel: design and cost analysis of hydrogen-based direct iron reduction.” *ChemRxiv*.

Rosner, F., D. D. Papadimas, K. P. Brooks, K. Yoro, R. K. Ahluwalia, T. Autrey, and H. Breunig. 2023b. “Green steel: design and cost analysis of hydrogen-based direct iron reduction.” *Energy & Environmental Science*, <https://doi.org/10.1039/D3EE01077E>.

Satyapal, S. 2022. *2022 AMR Plenary Session*. DOE. https://www.hydrogen.energy.gov/docs/hydrogenprogramlibraries/pdfs/review22/plenary4_satyapal_2022_o.pdf.

Statista. 2023. *Ammonia production in the United States from 2014 to 2022*. <https://www.statista.com/statistics/982841/us-ammonia-production/>. Online; accessed July 2023.

Terry, J., C. Gamage, N. Yavorsky, and R. Wilmoth. 2023. *Unlocking the First Wave of Breakthrough Steel Investments in the United States*. Technical report. <https://rmi.org/insight/unlocking-first-wave-of-breakthrough-steel-investments-in-the-united-states/>.

Transportation Statistics, B. of. 2023. *Average Freight Revenue per Ton-Mile*. <https://www.bts.gov/content/average-freight-revenue-ton-mile>. Online; accessed May 2023.

Tripp, C., D. Guittet, A. Barker, J. King, and B. Hamilton. 2019. *Hybrid Optimization and Performance Platform (HOPP)*, November. <https://www.osti.gov/biblio/1882832>.

U.S. Department of Energy. 2006. *Potential Roles of Ammonia in a Hydrogen Economy*. <https://www.energy.gov/eere/fuelcells/articles/potential-roles-ammonia-hydrogen-economy>.

———. 2024. *Achieving the Promise of Low-Cost Long Duration Energy Storage: An Overview of 10 R&D Pathways from the Long Duration Storage Shot Technology Strategy Assessments*. Technical report. U.S. Department of Energy, August. https://www.energy.gov/sites/default/files/2024-08/Achieving%20the%20Promise%20of%20Low-Cost%20Long%20Duration%20Energy%20Storage_FINAL_08052024.pdf.

Zaaijer, M., S. Kainz, J. Quick, M. S. de Alencar, S. S. P. Moreno, K. Dykes, C. Bay, and P. Bortolotti. 2024. *IEA Wind TCP Task 55: The IEA Wind 740-10-MW Reference Offshore Wind Plants*. Technical report. National Renewable Energy Laboratory NREL.